## **ARTICLE**

## Swelling characteristics of DNA polymerization gels

Joshua Fern,†a Ruohong Shi,†a Yixin Liu, a Yan Xiong, a David H. Gracias \*a-g and Rebecca Schulman \*abgh

Received 00th January 20xx, Accepted 00th January 20xx

DOI: 10.1039/x0xx00000x

The development of biomolecular stimuli-responsive hydrogels is important for biomimetic structures, soft robots, tissue engineering, and drug delivery. DNA polymerization gels are a new class of soft materials composed of polymer gel backbones with DNA duplex crosslinks that can be swollen by sequential strand displacement using hairpin-shaped DNA strands. The extensive swelling can be tuned and terminated using physical parameters such as salt concentration and biomolecule design. Previously, DNA polymerization gels have been used to create shape-changing gel automata with a large design space and high programmability. Here we systematically investigate how the swelling response of DNA polymerization gels can be tuned by adjusting the design and concentration of DNA crosslinks in the hydrogels or DNA hairpin triggers and the ionic strength of the solution in which swelling takes place. We also explore the effect hydrogel size and shape have on the swelling response. Tuning these variables can alter the swelling rate and extent across a broad range of variables, and provide a quantitative connection between biochemical reactions and macroscopic material behavior.

#### Introduction

Hydrogels are critical components of biological implants, drug delivery and tissue constructs, and soft robots. 1-4 Responsive hydrogels can change their volume significantly in response to environmental alterations, such as pH, light, and temperature, based on the absorption or release of water. 5-7 More recently, hydrogels have been developed that can swell or dissolve in response to biomolecular signals such as enzymes, antibodies, and nucleic acids. 8-11

Most structures in which responsive hydrogels are integrated require a specific speed and extent of response. Thorough characterization of the temperature-dependent swelling of poly(N-isopropylacrylamide) (PNIPAM) enabled the construction of pNIPAM-

based robotic actuators and devices for robotics and biomedical applications.  $^{\rm 12-15}$ 

Here, we investigate the factors that can be used to tune the extent of polymerization gel expansion in response to DNA sequence triggers. DNA-based hydrogels are especially promising for biomedical applications due to DNA's innate biocompatibility and large and continuing-to-be-developed set of tools/controllers for interfacing with other biomolecules that can direct their shape or size change. 16-18 DNA-crosslinked hydrogels that respond to temperature, ions, and small molecules have been reported. This work focuses on DNA-crosslinked polyacrylamide hydrogels, termed polymerization hydrogels, that can expand up to 100-fold volumetrically because of the sequential incorporation of DNA hairpins into their DNA crosslinks (Figure 1a). 19-22 Since then, we developed a family of these DNA polymerization gels where each gel consists of a DNA duplex crosslinks and a polymer backbone made from mono/macromers such as acrylamide(Am), acrylamide-co-bisacrylamide (Am-BIS), poly(ethylene glycol) diacrylate (PEGDA), and gelatin-methacryloyl (GelMA).22-24 The resulting multi-component DNA polymerization gels have a broad range of mechanical properties and enhanced biocompatibility. We also developed gel photopatterning protocols for each hydrogel, making it possible to assemble these gels at micron-scale in custom shapes.

To achieve more complex movements of the hydrogel system, we designed a mechanism that allows reversible hydrogel shape change: one set of DNA triggers swelling, whereas another set triggers shrinking.<sup>25</sup> Using these triggers, gels with different polymer backbones can be reversibly actuated for multiple cycles. Finally, we have achieved the design and fabrication of microscale devices, *i.e.*, gel automata, that can utilize chemical systems for swelling and shrinking to control multi-directional, multi-step motion in cycles and transform into meaningful shapes such as letters of the alphabet or numbers.

<sup>&</sup>lt;sup>a</sup> Department of Chemical and Biomolecular Engineering, Johns Hopkins University, Baltimore, MD 21218, United States of America;

<sup>&</sup>lt;sup>b</sup> Laboratory for Computational Sensing and Robotics (LCSR), Johns Hopkins University, Baltimore, MD 21218, United States of America; <sup>c</sup> Center for MicroPhysiological Systems (MPS), Johns Hopkins University, Baltimore,

MD 21218, United States of America;
<sup>d</sup> Department of Oncology, Johns Hopkins School of Medicine, Baltimore, MD 21218,

United States of America;

c Sidney Kimmel Comprehensive Cancer Center (SKCCC), Johns Hopkins School of

Medicine, Baltimore, MD 21218, United States of America;

f Department of Materials Science and Engineering, Johns Hopkins University,

Baltimore, MD 21218, United States of America;

<sup>9</sup> Department of Chemistry, Johns Hopkins University, Baltimore, MD 21218, United

States of America;

h Computer Science, Johns Hookins University, Baltimore, MD 21218, United States of

 $<sup>^{</sup>h}$  Computer Science, Johns Hopkins University, Baltimore, MD 21218, United States of America.

<sup>†</sup> Equal contribution.

<sup>\*</sup> Corresponding author. Email: <a href="mailto:rschulm3@jhu.edu">rschulm3@jhu.edu</a>; dgracias@jhu.edu. Electronic Supplementary Information (ESI) available. See DOI: 10.1039/x0xx00000x

ARTICLE Journal Name

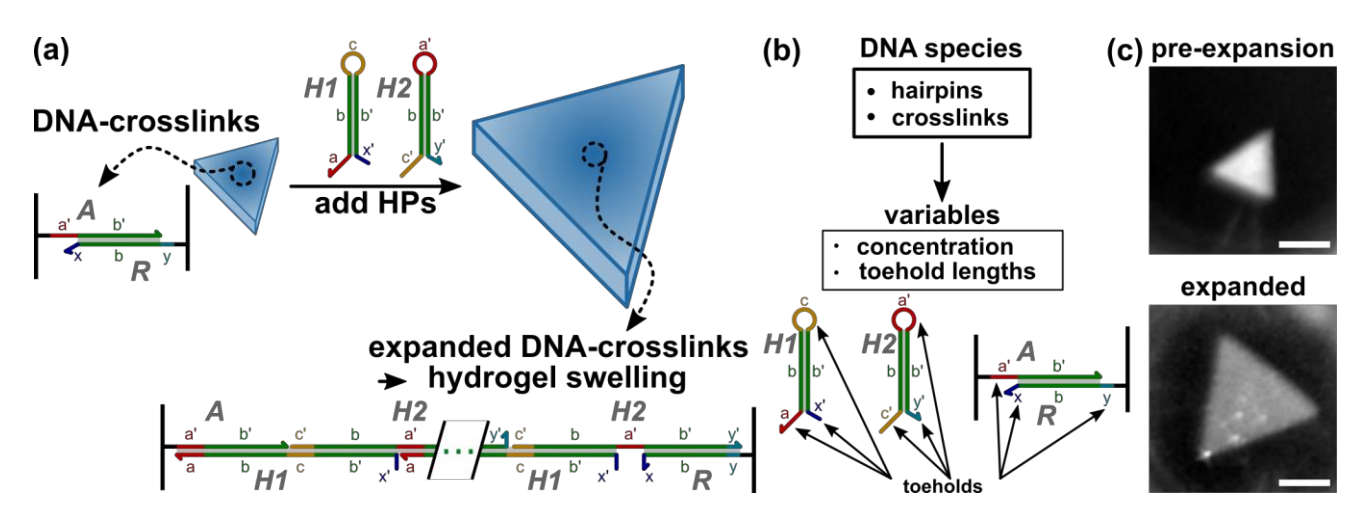


Figure 1. Schematic of DNA polymerization gel swelling using DNA hairpins, and tuning swelling by varying the concentrations or sequences of the DNA hairpins or crosslinks. (a) The hydrogels contain anchored DNA crosslinks that initiate the hybridization chain reaction (HCR) in which DNA hairpins polymerize. DNA hairpins sequentially incorporate into crosslinks, thus extending the resulting chain, significantly increasing the DNA content with the hydrogel. (b) Variables that could control the rate and degree of DNA-induced hydrogel swelling. (c) Representative optical images of a poly(PEGDA10k-co-S1dsDNA1.154) hydrogel expanded using 20 µM of each hairpin (H1 and H2) before and after polymerization. Hydrogels are visualized using Rhodamine B methacrylate that is incorporated during polymerization (See Methods). Scale bars: 1 mm.

The swelling process of DNA polymerization gels is triggered by DNA hairpins approximately 50-70 bases in length (Figure 1a). DNA hairpins insert into the hydrogel via a strand displacement reaction between a DNA hairpin and the DNA crosslink or growing DNA chain.<sup>22,26</sup> The thermodynamics and kinetics of strand displacement reactions are well-studied, and the dependence of these parameters on the lengths and sequences of the different domains of the hairpin and crosslink sequences have been elucidated.<sup>27–29</sup> For example, the lengths of the toeholds can determine the rate of the insertion reaction across multiple orders of magnitude and can be tuned independently of the thermodynamics (*i.e.*, the energy change) of the reaction.<sup>27,28</sup> The ionic strength has also been shown to affect the rate of DNA strand displacement.<sup>28,30</sup>

Here, DNA strand displacement occurs inside a hydrogel network, and its procession is coupled to a change in network size and density. We sought to understand how the thermodynamics and kinetics of the chemical reaction that governs insertion affect the rate and extent of the hydrogel swelling process. To do so, we systematically investigated how different features of the DNA polymerization process affect how quickly and how much swelling of hydrogels occurs. We study the DNA-directed swelling of photopatterned PEG-co-DNA hydrogels.<sup>23</sup> These hydrogels have both covalent crosslinks between PEG chains that are not stimulus-responsive and DNA crosslinks that respond to specific DNA signals. We measure variations in the swelling rate and extent of these PEG-co-DNA hydrogels that result from changes in the thermodynamics and kinetics of the DNA strand displacement reactions that drive swelling.

We investigate how the concentrations of the DNA crosslinks and DNA hairpins and domain lengths on the hairpins that initiate strand displacement affect swelling. Well-mixed solution kinetics would predict that the flux of polymerization, and thus the rate of swelling, should be proportional to the product of crosslink and hairpin concentrations.<sup>31</sup> We also consider the effect of toehold sequence on the swelling process. Toehold sequence and length are known to be primary determinants of the kinetics of both 2-way and 4-way toehold-mediated branch migration processes, where in 2-way branch migration, the log of the forward rate of interaction is

proportional to toehold length.<sup>27,28,32</sup> We then consider the influence of salt concentration since the kinetics and thermodynamics of the DNA polymerization process that drives swelling could be affected by cation type and concentration (as could the degree of polymer network expansions).<sup>30,33</sup> Given that the PEG gels expand considerably despite the constraints on network topology induced by the PEG-PEG chain crosslinks, we test whether DNA-directed swelling could occur in other means besides the extension of crosslinks. Finally, we explored the impact of morphological attributes on the reaction kinetics as the materials' diffusion time is reliant on the shape and size.<sup>34</sup>

Our results suggest that the amount of energy expended in the polymerization of crosslinks has a direct and proportional effect on the amount of swelling of the hydrogels. The rate of polymerization can also affect the rate of swelling. However, given the interplay of the polymerization reaction and other reactions and forces involving the DNA strands, polymer network, and ions, a quantitative theory for tuning these forces by designing DNA must take all of these factors into account.

#### Results

**PEG-co-DNA polymerization hydrogels.** In this paper, we utilized PEG-co-DNA polymerization hydrogels in our studies. The macromer, polyethylene glycol diacrylate (PEGDA10k, Mn 10,000), was used for building the base polymer matrix. Due to the presence of two acrylate moieties on each end of the PEG chain, PEGDA can form a polymer network through free radical-initiated chain polymerization without the presence of DNA crosslinks.<sup>23,35</sup> This property enables us to vary the amount and form of DNA (e.g., single-stranded or double-stranded) anchored inside the gel without compromising the integrity of the polymer network. We used a double-stranded DNA complex (dsDNA) composed of annealed A and R strands that were both short, synthetic DNA and were purchased from IDT as a DNA hybridization chain reaction (HCR) initiator. [dsDNA] refers to the concentration of the double-stranded DNA complex, which is the same as the concentrations of A and R strands. We first polymerized

Journal Name ARTICLE

PEGDA10k hydrogels using a pre-gel solution containing 1.154 mM of the dsDNA into equilateral triangle-shaped gel sheets (1 mm in side length and 160 µm in thickness) using a previously developed hydrogel photopatterning method.<sup>22,23</sup> All studies in this work used this structure to measure swelling rate and extent unless otherwise stated. Briefly, the photopatterning chamber consists of a chromium (Cr) CAD photomask and a glass substrate, with 160 µm spacers that control the height of the gels. During photopatterning, the pre-gel solution, which contains the PEGDA macromers, acrydite-modified DNA crosslinks, photoinitiator, and fluorophore, was exposed to UV light through the transparent parts of the Cr mask and thus cured. Photopatterning the structures used in our study allowed the use of gels of precisely the same sizes for comparison, minimizing one potential source of variability in swelling behavior. We first verified that the poly(PEGDA10k-co-S1dsDNA1.154) hydrogels expanded in response to DNA by incubating the hydrogels in a DNA hairpin solution. This solution used for swelling contained 20  $\mu M$  of each of two DNA hairpins, H1 S1 6/3 and H2 S1 6/3 (sequence set 1, Supp. Table 1), which was previously shown to incorporate into the DNA crosslinks via insertion polymerization. 22,26 The volume of the DNA hairpin solution used for each triangle-shaped gel sheet swelling was 100 μL, while the volume of the as-made gel is about 0.08 μL. There are roughly 30 times more DNA hairpins in the solution as a whole than there are DNA crosslinks, which are only inside the gel (Supp. Text 1). The gels maintained their triangular shape and expanded more than 6-fold in volume after 60 hours of hairpin incubation (Figure 1c). No swelling behaviour was observed when only buffer or the wrong sequences of DNA hairpins were present (Supp. Fig. 1a).

Variation of swelling with altering DNA crosslink and hairpin concentrations. We used the PEG-co-DNA gels to investigate the effect of DNA crosslink concentration on the degree and rate of DNAinduced hydrogel swelling. We prepared poly(PEGDA10k-co-S1dsDNA) hydrogels using pre-gel solutions containing 0.250, 0.750, or 1.154 mM double-stranded DNA crosslinks (A S1 and R S1) and incubated each of the hydrogels with 20  $\mu M$  of each of the set 1 sequence hairpins, H1\_S1\_6/3 and H2\_S1\_6/3 (Figure 2a). We plotted the swelling ratio  $\Delta$  L/L<sub>0</sub> (the change in the side length with respect to the original side length L<sub>0</sub>) as a function of time (hours). The initial rates of swelling, i.e., the average rate of swelling per hour over the first two hours, were 0.020±0.002, 0.064±0.007, and 0.046±0.002 (± represents standard error), respectively, for the three crosslink concentrations (0.250, 0.750 and 1.154 mM dsDNA anchors respectively) calculated using MATLAB's polyfit function. This data suggest that lower crosslink concentrations reduce the rate of swelling but do not fit any definite trend, perhaps because the initiation rate is subject to variation because of mixing time, and relatively few data points are used to estimate the slope. The relative changes in side length after 60 hours of incubation with hairpins, which we chose as an approximation to the final state swelling extent, were 0.23±0.03, 0.65±0.17 and 0.82±0.06 (95% confidence interval) for hydrogels containing 0.250, 0.750 and 1.154 mM dsDNA crosslinks respectively. These extents suggest that the total swelling is roughly linear in the crosslink concentration over the range of concentrations tested. Such a result would be consistent with the idea that DNA hairpins are in excess in these experiments so that each crosslink swells to roughly the same extent regardless of crosslink concentration and each crosslink contributes roughly the same amount on average to the extent of the swelling increase of the hydrogel.

The above argument assumes that DNA hairpins are in excess, so raising the hairpin concentration should not affect the final extent of

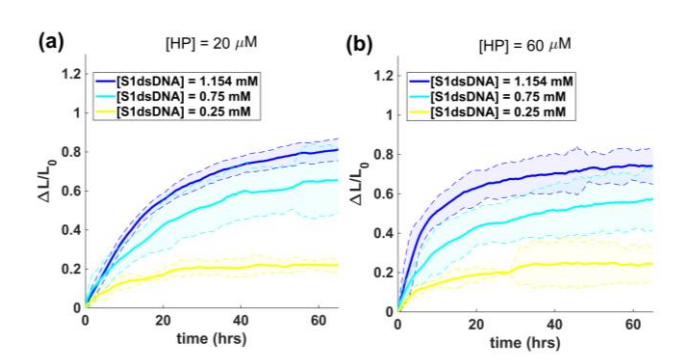


**Figure 2.** Rates and extent of poly(PEGDA10k-co-S1dsDNA) hydrogel swelling for different crosslink and hairpin concentrations. Hydrogels were polymerized with DNA crosslinks at 1.154, 0.750, or 0.250 mM (sequence set 1) and were incubated with hairpins at a final concentration of (a) 20  $\mu$ M or (b) 60  $\mu$ M H1 and H2 (sequence set 1, H1\_S1\_6/3 and H2\_S1\_6/3). Curves are the relative change in hydrogel side length after the addition of hairpins. Solid lines are the average of 3-6 hydrogels; dashed lines show 95% confidence intervals as determined by standard deviations.

swelling. A higher hairpin concentration could, however, affect the rate of achieving that extent by speeding up the rate of polymerization at crosslinks. We evaluated these hypotheses by repeating the swelling of PEGDA hydrogels with different concentrations of crosslinks but with 60  $\mu$ M (rather than 20  $\mu$ M) of each hairpin type (Figure 2b). Both the initial rate and total extent of swelling were roughly proportional to the crosslink concentration in these experiments: The initial rates of swelling in the first 2 hours were 0.029±0.001, 0.065±0.005, and 0.087±0.001 (standard error), and total extents of swelling were 0.24±0.07, 0.58±0.17, and 0.74±0.09 (95% confidence interval) for 0.250, 0.750 and 1.154 mM of crosslinks respectively.

While faster swelling occurred in the first 10 hours, the final extent of hydrogel swelling was roughly the same when 60  $\mu$ M of hairpins were added to the solution vs. when 20  $\mu$ M of hairpins were added to the solution. This observation is consistent with the idea that the hairpins were in excess, and the total number of crosslinks limited the extent of swelling.

Self-limiting polymerization at crosslinks with terminator hairpins reduces swelling extent but can increase swelling speed. DNA hairpins facilitate continuous swelling in poly(Am-co-DNA) gels<sup>22</sup>. Swelling can also reach a specific extent at steady state through the use of terminator hairpins that can polymerize at crosslinks, much as the polymerizing hairpins do.<sup>22,23</sup> These terminator hairpins have non-complementary loop domains that, once inserted, prevent the insertion of subsequent hairpins (Supp. Text 2) such that the final extent of uniaxial swelling is roughly inversely proportional to the fraction of terminator hairpins or the expected final average length of the crosslink in polymer units.<sup>22</sup> In PEG gels, crosslink extension may be limited even in the absence of these terminators by covalent linkages in the network that make crosslink extension unfavourable beyond some distance. We next asked how the presence of terminator hairpins affected the rate and extent of DNA-directed swelling. characterized poly(PEGDA10k-cohvdrogel We S1dsDNA1.154) hydrogel swelling induced by DNA hairpins with 2 or 10% mole fraction of terminator hairpins (H1 S1 ter and H2 S1 ter)

ARTICLE Journal Name

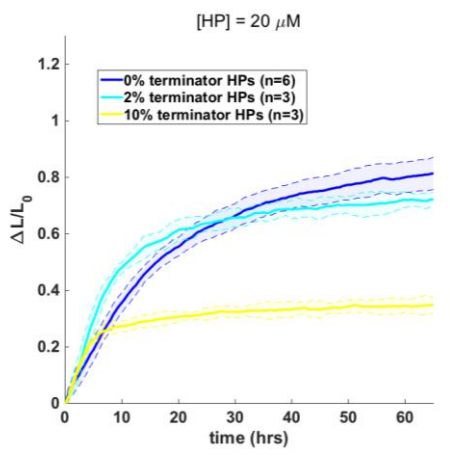


Figure 3: Terminator hairpins can reduce the extent of hydrogel swelling with more terminators causing further reduction. The relative change in side length of poly(PEGDA10k-co-S1dsDNA1.154) hydrogel triangles incubated with set 1 hairpins (H1\_S1\_6/3 and H2\_S1\_6/3, H1\_S1\_ter and H2\_S1\_ter) at a total of 20  $\mu$ M per hairpin type. Solid curves are each the averages of measurements of six or three hydrogels. Dashed lines show 95% confidence intervals as determined by standard deviations.

and compared it to the rate of hydrogel swelling in the presence of the same concentration of hairpins without any terminators (Fig. 3). When both 2% and 10% terminators were added, the extent of swelling was reduced with respect to the extent of swelling in hairpin solution without terminators. The overall change in the trend of swelling extent on the inclusion of terminators is consistent with that observed elsewhere. For the reported poly(Am-co-DNA) gels, the change in side length over original side length ( $\Delta$  L/L0) for 0, 2, and 10% terminator are 3.8, 2.6, and 0.8, while the values for PEG gel are 0.82, 0.72, and 0.34.

Interestingly, we also observed a slight increase in the initial rate of swelling when terminators were used, also consistent with previous studies.<sup>22</sup> This initial increase in rate could be due to terminating the extension of crosslinks at the hydrogel surface requires that hairpins incorporate into crosslinks deeper within the hydrogel, perhaps ensuring more even and thus faster swelling when measured by the size of the material as a whole. The inclusion of terminators can also reduce unwanted hairpin nucleation in the solution, reducing the size of DNA complexes and facilitating diffusion. Generally, terminators could be used to control the size of a PEG-co-DNA gel after DNA-directed swelling, and our results are consistent with the ability to achieve a wide range of final sizes by adjusting the terminator proportion.

Effect of toehold length on hydrogel swelling. We next asked how the reaction rate and energy balance between the hairpins and crosslinks might be used to control the rate and extent of DNAdirected swelling, as varying the lengths of the toeholds on the hairpins and crosslinks would alter the kinetics and thermodynamics of the extension reaction.<sup>27,28</sup> Because hairpins and crosslinks react via a toehold-mediated 4-way branch migration, there are 2 toeholds (termed primary, Fig 4a, and secondary, Fig 5a) involved in the process that could each affect insertion reaction kinetics and thermodynamics. In our initial experiments, the primary toehold was 6 nucleotides long and the secondary toehold was 3 nucleotides long. We began by investigating how lengthening the primary toehold would change the speed and extent of DNA-directed swelling. We designed a set of DNA crosslinks, termed sequence set 2, with 10 nucleotide-long primary initiating toeholds on one of the crosslink strands that could hybridize primary toeholds of up to these lengths (A S2 and R S2, set 2 v1, Supp. Table 1).

The hydrogels containing set 2 crosslinks swelled at a slightly slower rate, and a lower final degree in response to the same concentration of hairpins with the same toehold lengths compared to set 1 (Supp. Fig. 12). Hydrogels containing set 2 crosslinks achieved

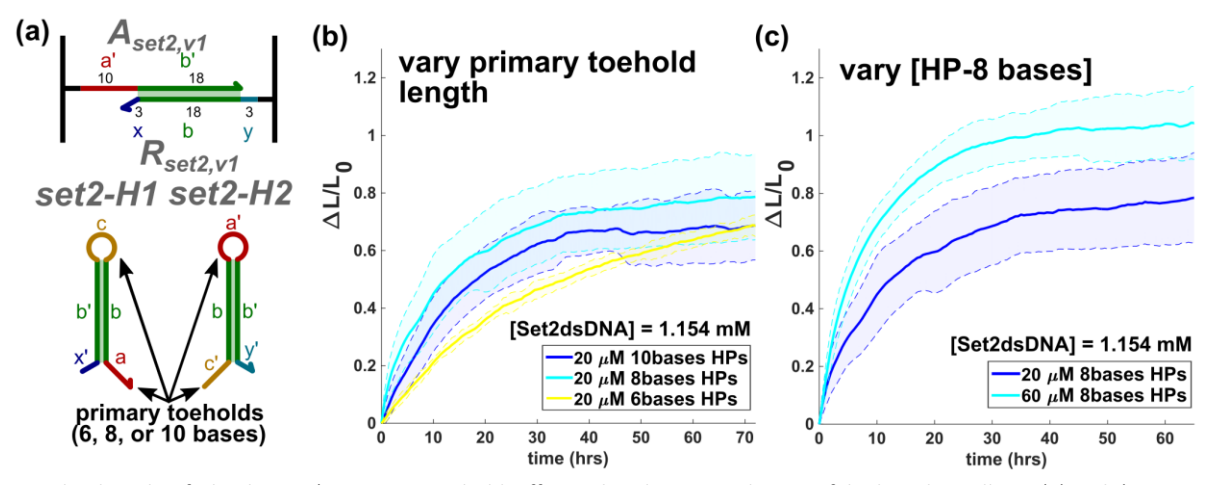


**Figure 4**. The length of the hairpin's primary toehold affects the degree and rate of hydrogel swelling. (a) Poly(PEGDA10k-co-S2\_v1dsDNA1.154) hydrogels were polymerized with crosslinks containing 10bases primary toeholds and 3bases secondary toeholds. Numbers indicate the number of bases in those domains in the crosslink. Hairpins were designed to have 6-, 8-, or 10- base long primary toeholds that can react with the crosslinks for hairpin insertion. (b) Relative change in hydrogel side length for hydrogels polymerized with 1.154 mM of the crosslinks in (a) incubated with 20 μM of hairpins containing 6- (H1\_S2\_6/3 and H2\_S2\_6/3), 8- (H1\_S2\_8/3 and H2\_S2\_8/3), or 10- (H1\_S2\_10/3) and H2\_S2\_10/3) base long primary toeholds. (c) Relative change in hydrogel side length for hydrogels polymerized with 1.154 mM of the crosslinks in (a) incubated with 20 or 60 μM 8 bases primary toehold hairpins (H1\_S2\_8/3 and H2\_S2\_8/3). Solid lines are the average of 3 to 5 hydrogels; dashed lines show 95% confidence intervals as determined by standard deviations.

Journal Name ARTICLE

an average relative change in hydrogel side length of about 0.65 in 60 hours compared to a relative change of 0.8 for hydrogels containing sequence set 1 crosslinks. This difference is potentially due to differences in the two sets' sequences: there is only one G/C pair in both primary and secondary initiating toeholds of the set 2 sequence, while the set 1 crosslink sequence contains three G/C pairs. Toeholds with a lower G/C content have a less negative  $\Delta$  G of hybridization, leading to a slower rate of strand displacement.  $^{28,36}$ 

We used the set 2\_v1 crosslinks to measure the difference in swelling rate and extent when hairpins with 6, 8, or 10 base primary initiating toeholds direct swelling (H1\_S2\_6/3 and H2\_S2\_6/3, H1\_S2\_8/3 and H2\_S2\_8/3, H1\_S2\_10/3 and H2\_S2\_10/3, Figure 4a). Hydrogels incubated with hairpins with 8- and 10-base long primary toeholds swelled slightly faster and to a greater extent by 70 hours than the hydrogels incubated with hairpins with 6 base- primary toehold (Figure 4b). These slight differences are consistent with studies of 4-way branch migration, in which slight increases (on the order of 2-fold) in reaction rate are observed when extending either the primary or secondary toehold length to more than 4-5 bases.<sup>27,37</sup> The relatively large size of the loop (10 bases) in the 10-base primary toehold hairpin could allow undesired hairpin-hairpin polymerization

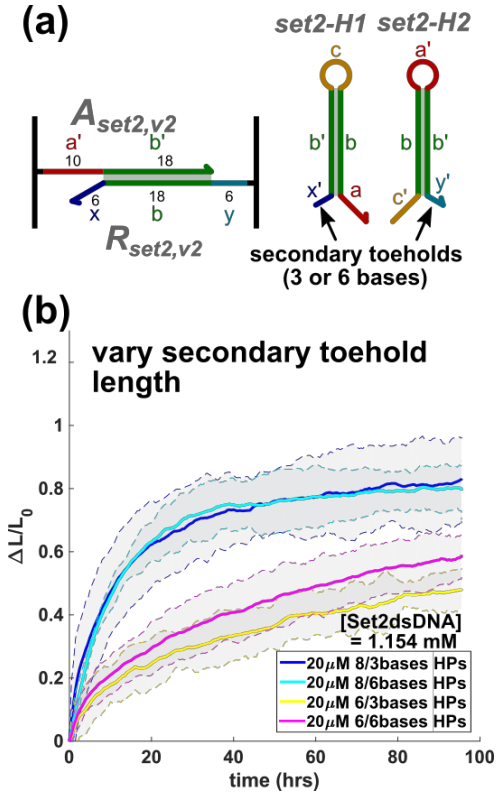


**Figure 5.** Effect of the length of the hairpin's secondary toehold on the degree and rate of hydrogel swelling. (a) Poly(PEGDA10k-co-S2\_v2dsDNA1.154) hydrogels were swollen by hairpins with different primary and secondary toehold lengths. (b) Relative change in hydrogel side lengths of hydrogels polymerized with 1.154 mM crosslinks in (a) incubated with 20  $\mu$ M of hairpins with different primary/secondary toehold lengths (in bases). Solid lines are the average extents of swelling of 3 hydrogels; dashed lines show 95% confidence intervals as determined by standard deviations.

reactions,<sup>36</sup> leading to a slight decrease in the effective hairpin

concentration and the overall rate of insertion into the crosslinks. Interestingly, unlike poly(PEGDA10k-co-S1dsDNA1.154) hydrogels incubated with 6 base-long primary toehold hairpins (Figure 2), poly(PEGDA10k-co-S2\_v1dsDNA1.154) hydrogels incubated with 8 base-long primary toehold hairpins had an extent of swelling that was dependent upon hairpin concentration (Figure 4c). The rate and the extent of swelling of poly(PEGDA10k-co-S5dsDNA1.154) hydrogels increased when the concentration of 8 base-long primary toehold hairpins was increased from 20  $\mu$ M per hairpin to 60  $\mu$ M per hairpin. Poly(PEGDA10k-co-S2dsDNA1.154) hydrogels reached a uniaxial swelling ratio greater than 1 within 24 hours of incubation with 60  $\mu$ M per hairpin.

Since increasing the length of the primary toehold from 6 to 8 bases led to a moderate increase in the rate and extent of hydrogel swelling, we hypothesized that increasing the length of the secondary toehold on the hairpins and crosslinks could increase the rate and extent of swelling even further. To examine the effect of changing the length of the secondary toehold domain, we designed a variant of the sequence set 2 crosslink v2, which had a 6- base long domain for binding a secondary toehold in addition to the 10- base long domain for binding a primary toehold (A S2 and R S2x6, Figure 5a, Supp. Table 1). We then measured the extent of swelling of poly(PEG-co-S2 v1dsDNA1.154) hydrogels when incubated with 20 μM hairpins with 6 base-long secondary toeholds and either 6 or 8 base-long primary toeholds (H1\_S2\_8/6 and H2\_S2\_8/6, H1\_S2\_6/6 and H2\_S2\_6/6 Figure 5b). The length of the secondary toehold was not increased beyond 6 bases because equilibrium analysis using NUPACK showed an increase in hybridization between complementary secondary toeholds (e.g., x to x' in Figure 1a) longer than 6 bases at the insertion site that could inhibit hairpin insertion.

Increasing the lengths of the secondary toeholds from 3 to 6 bases resulted in a slight but not statistically significant increase in the degree of hydrogel swelling. No increase in the rate of swelling was observed. In contrast, in studies of 4-way branch migration with a 6base long primary toehold in which the secondary toehold length was increased from 4 to 6 bases, at least 4-fold increases in the reaction rate constant were observed and the  $\Delta G^{o}$  for the reaction decreased from either -8.63 or -10.23 kcal/mol to -12.45 kcal/mol.<sup>27</sup> These results and those in Figure 4 suggest that the kinetics of branch migration in crosslinked hydrogels, where molecular crowding is a factor, may occur following different dependencies than those occurring in free solution. For example, recent studies have shown that the  $\Delta G^{\varrho}$  of DNA hybridization decrease by up to 50% in 40wt% PEG solutions.<sup>38</sup> There is, however, little data about kinetic parameters, and the rates of 4-way toehold branch migration even in solution are much less well-studied than other toehold-mediated branch migration processes. More studies would likely be needed on both types of processes to establish a systematic comparison.

**Salt concentration.** Like toehold length, the concentration and type of cations in solution are also strong determinants of the kinetics and thermodynamics of DNA strand displacement and toehold-mediated branch migration.  $^{28,30}$  A commonly accepted model is that the  $\Delta G^{\circ}$  of DNA hybridization increases with the log of cation (either Na+ or Mg²+) concentration and that these increases occur per pair of bases and are well-modeled by the nearest neighbor model of DNA hybridization.  $^{39,40}$  The salt concentration would therefore be expected to change the extent of swelling and possibly the rate of swelling.

We tested the swelling of poly(PEG-co-S2dsDNA1.154) hydrogels in several different sodium concentration buffers (1x TAE/1.25mM Mg<sup>2+</sup>, 1x TAE/1.25 mM Mg<sup>2+</sup>/100 mM Na<sup>+</sup>, 1x TAE/1.25 mM Mg<sup>2+</sup>/500

ARTICLE Journal Name

mM Na+, 1x TAE/1.25 mM Mg<sup>2+</sup>/1000 mM Na+, 1x TAE/1.25 mM Mg<sup>2+</sup>/2000 mM Na<sup>+</sup>). To control for the effects of ion-dependent swelling of the PEG matrix, we initially incubated each hydrogel in each buffer for at least 24 hours before adding 20 µM of each DNA hairpins (H1\_S2\_6/3 and H2\_S2\_6/3). The results in Figure 6 indicate that the initial rate and the extent of swelling after 80 hours increased with an increasing Na<sup>+</sup> concentration in the range of 0 mM to 500 mM. Furthermore, the swelling behaviour of gels in 2M Na<sup>+</sup> was similar to that of 500 mM Na<sup>+</sup>, 1 M Na<sup>+</sup>, and the control group using 1x TAEM. We also tested the swelling of poly(PEG-co-S1dsDNA1.154) hydrogels in several different buffers: 1x TAEM, 1xTAE/100mM Na+, 1x sodium phosphate-sodium chloride (SPSC, 1 M NaCl, 50 mM Na<sub>2</sub>HPO<sub>4</sub>; pH 7.5) and PBS (Supp. Fig. 1). No significant further swelling due to the ions alone was observed. Our measurements indicate that the hydrogels incubated with 1x TAEM and 1xSPSC exhibit similar rates and extents of swelling, while the rates and extents of swelling of hydrogels in TAE/Na<sup>+</sup> and PBS were significantly lower. SPSC has a higher concentration of sodium (1 M) than either PBS (137 mM) or TAE/100 mM Na+, so would be expected to allow stronger DNA hybridization as would TAE/12.5 mM Mg<sup>2+</sup> given the comparative effects of  $Mg^{2+}$  and  $Na^{+}$  ions on hybridization thermodynamics. We further tested whether varying the concentration of Mg<sup>2+</sup> in TAEM would affect the swelling, and the result in Supp. Fig. 2 shows that the rate and degree of swelling were almost the same. This finding suggests that the amount of Mg<sup>2+</sup> can be adjusted as needed, for example, to deploy DNA polymerization gels in environments such as cell culture without significantly altering this type of DNA strand displacement process.

**Expanding hydrogels containing ssDNA anchors.** Finally, we asked whether hydrogel swelling could be induced by DNA hairpins with specific sequences when the hairpin polymerization initiators within the hydrogel were not crosslinks but single strands of DNA (Figure 7a). A single-stranded DNA initiator initiates the polymerization of the hairpins only through the primary toehold. Hairpin insertion then proceeds through a 3-way branch migration pathway rather than via 4-way branch migration reactions as in the case of the double-stranded initiator.

When polymerizing hairpins are added to hydrogels containing single-stranded DNA initiators, the hairpins should incorporate into the hydrogel as in the case with double-stranded initiator complexes. But when single-stranded initiators are used, this incorporation does not extend hydrogel crosslinks. Because the ssDNA is not anchored to the gel on both ends, it only indirectly, through mixing energy and excluded volume, alters the shape of the hydrogel network. If these effects are relatively unimportant for hydrogel swelling, less or even no hydrogel swelling might be expected to occur during such a process.

We prepared PEGDA10k hydrogels polymerized with either 0.750, 1.154, or 2.308 mM of the sequence set 2 A strand (A\_S2, Supp. Table 1), which contains the primary toehold (Figure 7a). We incubated these poly(PEGDA10k-co-S2ssDNA) hydrogels (sequence set 2 v1, Supp. Table 1) with 20  $\mu$ M 8-base primary toehold hairpins (H1\_S2\_8/3 and H2\_S2\_8/3). The hydrogels did swell, although to a lesser extent than when double-stranded crosslinks were used. The extent of hydrogel swelling was dependent upon the concentration of ssDNA initiators polymerized into the hydrogel (Figure 7b). When the hydrogels were incubated with 10 base primary toehold hairpins (H1\_S2\_10/3 and H2\_S2\_10/3), the relative changes in side length of poly(PEGDA10k-co-S2ssDNA) hydrogels were about 0.3 to 0.6 and 60 hours when the initiator concentrations were 1.154 mM to 2.308 mM respectively (Figure 7c). The roughly linear dependence of swelling

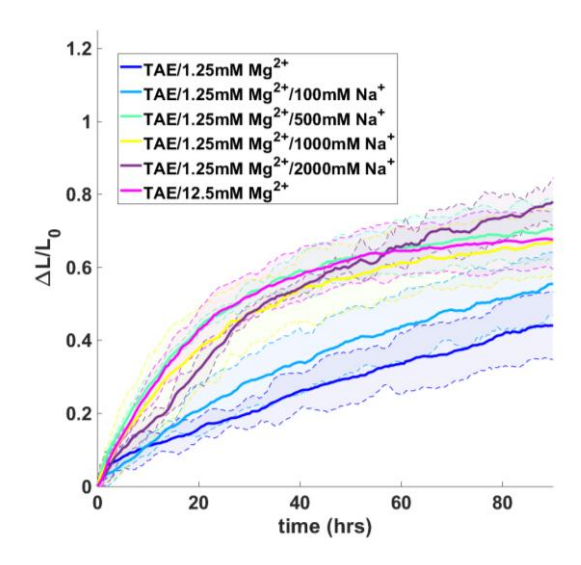


**Figure 6.** Swelling kinetics for poly(PEG-co-S2dsDNA1.154) hydrogel using 20  $\mu$ M of H1\_S2\_6/3 and H2\_S2\_6/3 in: 1x TAE/1.25mM Mg²+, 1x TAE/1.25mM Mg²+/100mM Na<sup>+</sup>, 1x TAE/1.25mM Mg²+/500mM Na<sup>+</sup>, 1x TAE/1.25mM Mg²+/2000mM Na<sup>+</sup>, and 1x TAE/1.25mM Mg²+ (TAEM). Solid curves are the averages of measurements of 3 hydrogels each. Dashed lines show 95% confidence intervals as determined by standard deviations.

extent on crosslink concentration in each experiment is consistent with the linear dependence on swelling extent from double-stranded crosslinks.

While the extent of swelling from double-crosslinks was not highly dependent on toehold length, poly(PEGDA10k-co-S2ssDNA1.154) hydrogels incubated with hairpins with 10 base primary toeholds (H1\_S2\_10/3 and H2\_S2\_10/3) swelled significantly more than those incubated with hairpins with 6- base (H1\_S2\_6/3 and H2\_S2\_6/3) or 8- base (H1\_S2\_8/3 and H2\_S2\_8/3) long primary toeholds (Figure 7d). Hydrogels swelled faster, however, when incubated with hairpins with 6 base primary toeholds. In the free solution, the rate of a 3-way branch migration initiated by 6 base toeholds is approximately 2 fold lower than those of 8 and 10 base toeholds (whose rates are indistinguishable). <sup>28</sup> The relative similarity of the rates of swelling in response to the hairpins with the 6 and 8 base toeholds are consistent with the rates of strand displacement reactions, but the slower rate of swelling of hydrogels in response to the hairpins with 10 base toeholds is not.

The hydrogels polymerized with the ssDNA initiators also showed a slight dependence upon the concentration of polymerizing hairpins added to the hydrogel. The change in side length of poly(PEGDA10k-co-S2ssDNA1.154) hydrogels increased from 0.15 to 0.23 in 50 hours when the concentration of 8 base primary toehold hairpins was increased from 20  $\mu M$  to 60  $\mu M$  per hairpin (Figure 7e). This change in the extent of swelling is consistent with the difference in the extent of swelling observed when the concentration of the same hairpin was varied with double-stranded crosslinks (Figure 4c).

We did a gel electrophoresis experiment to compare the extent of polymerization when the initiator is single-stranded vs. when it is double-stranded (Supp. Fig. 13). The extent of polymerization is less when using a single-stranded initiator than when using a double-

Journal Name ARTICLE

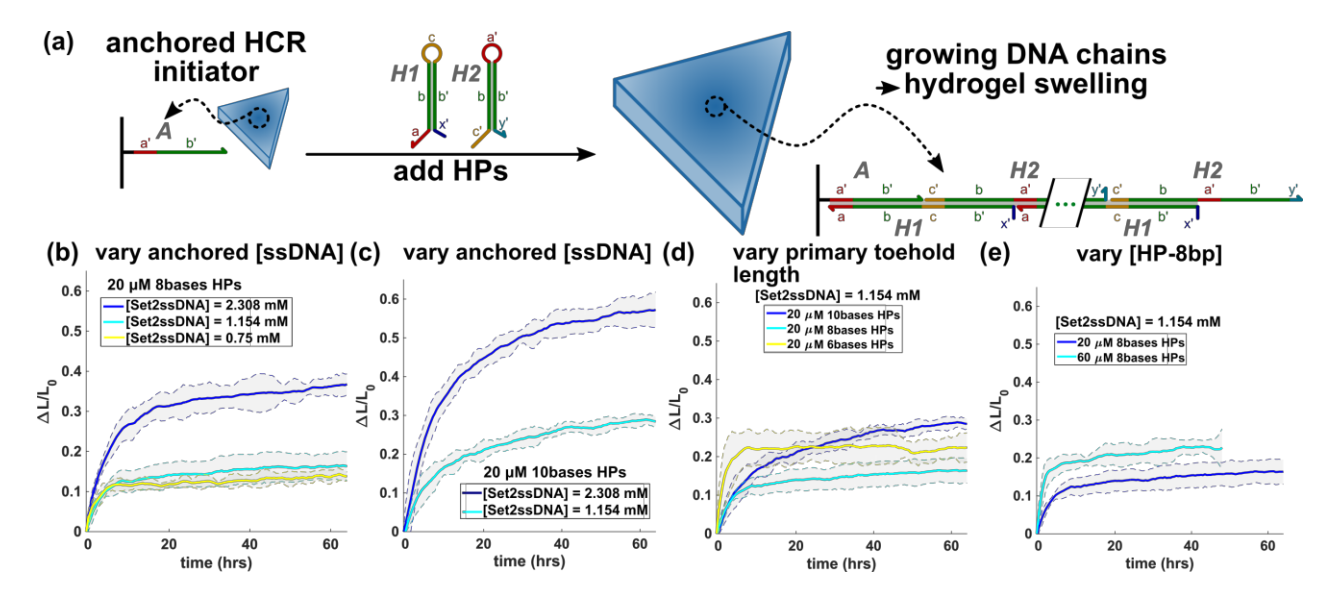


**Figure** 7. DNA-directed swelling of hydrogels with anchored single-stranded HCR initiators. (a) Single-stranded DNA that is capable of initiating an HCR process is anchored to hydrogels during hydrogel polymerization. Hairpins sequentially bind to these anchored DNA strands via a hybridization chain reaction, inducing hydrogel swelling. (b) Relative change in the side length of poly(PEG-co-S2ssA<sup>ac</sup>) hydrogels with varying concentrations of anchored ssDNA HCR initiators. Hydrogels were incubated with 20 μM of 8 bases long primary toehold hairpins. (c) Relative change in side length of poly(PEG-co-S2ssA<sup>ac</sup>) hydrogels with varying concentrations of anchored ssDNA HCR initiators incubated with 20 μM of 10bases long primary toehold hairpins. (d) Relative change in side length of poly(PEG-co-S2ssA<sup>ac</sup>1.154) hydrogels incubated with 20 μM hairpins with 6, 8, or 10 bases long primary toeholds. (e) Relative change in side length of poly(PEG-co-S2ssA<sup>ac</sup>1.154) hydrogels incubated with 20 or 60 μM 8bases primary toehold hairpins. Solid lines are the average of 3 to 5 hydrogels; dashed lines show 95% confidence intervals as determined by standard deviations.

stranded initiator. Further, in both cases, there is an abundance of leftover hairpin monomers. This observation could be explained by the fact that the polymerization step from a single-stranded initiator is less forward-driven than the polymerization step from a double-stranded initiator is, due to the absence of the toeholds x and y in the R strand when a single-stranded initiator is used.

Dependence of design rules on hydrogel form. To explore whether the size of the hydrogel affects the degree of swelling, we fabricated hydrogel triangles with the same side length (1 mm) and varying thicknesses of 60  $\mu m,\,160~\mu m$  (as used in other gels in this paper for comparison), and 320 µm. The final swelling characteristics showed that the 60 µm- thick gel had swelled approximately 30% more after 40 hours as compared to the 160 μm- thick gels, while the 320 μmthick gels had swelled considerably less (Supp. Fig. 3). This reduction of swelling with increasing gel thickness could be due to a higher crosslinking density in the thicker gels as considerably more energy was used to polymerize the 320  $\mu m$ - thick gels during photopatterning than was used to pattern the thinner gels (1200 mJ/cm<sup>2</sup> vs. 600 mJ/cm<sup>2</sup>). The lesser extent of swelling in thicker gels could also be due to the hairpins not penetrating all the way into the 320 µm-thick gels, causing more swelling on the borders of the gels, preventing overall area expansion. Such inhomogeneous swelling was observed with Am-DNA gel particles with a 1 mm diameter during swelling (Supp. Video 1 and 2). Both videos show that the swelling happens successively from outside to inside of a material, while increasing the terminator percentage from 2% to 10% increases the rate of swelling in the interior part of the gel particle. The initial rates of swelling of the 60  $\mu$ m- and 160  $\mu$ m- thick gels were largely the same, which indicates that diffusion is not a major speed-limiting factor during the swelling process of thinner gels. However, the

swelling process of a thicker (320  $\mu$ m) gel could be diffusion-limited as the Damköhler number (Da) is a quadratic function of thickness. The Damköhler number (Da) is a dimensionless quantity used in chemical engineering and fluid mechanics to characterize the relative rates of reaction and diffusion or transport processes in a system. As Da = (Diffusion time) / (Reaction time), high Da values indicate a diffusion-limited distribution.

To examine the extent to which the swelling process depends on the shape of the hydrogel, we repeated some comparisons using millimeter-scale hydrogel particles. PEGDA10k hydrogel particles with diameters of about a millimeter containing different concentrations of S1dsDNA crosslinks were prepared using a previously developed droplet-based synthesis method.<sup>24</sup> As expected, the DNA-directed swelling of the hydrogel particles was slower than the swelling of the smaller triangles, making the final extent of swelling of the particles challenging to discern in some cases. The measured extents of swelling of the particles were also somewhat more varied than the measured extents of swelling of the triangles. This variation may be due to the fact that the particles have slight aberrations from a spherical shape so that rotations of the particles change their apparent sizes. As photopatterned gels offer improved consistency and reproducibility in conducting gel swelling assessments, we suggest employing this fabrication technique in future gel swelling characterization studies.

Nonetheless, the measurements on the extent of swelling of the particles showed trends with respect to DNA concentration and crosslink form that were qualitatively similar to those observed in experiments with hydrogel triangles while having larger sample variance (Supp. Fig. 4 and 5). Salinity also affected the swelling kinetics for gel particles, where hairpins in 1x TAEM and 1x SPSC

ARTICLE Journal Name

buffer performed similarly while better than TAE/Na $^{\scriptscriptstyle +}$  and PBS (Supp. Figs. 6 and 7).

We also prepared poly(PEGDA10k-co-S1dsAacRno-ac1.154) hydrogel particles where the AR complex (see Figure 1a) was covalently linked to the PEGDA matrix only through the A strand. Interestingly, the particles swelled at essentially the same rate and extent as poly(PEGDA10k-co-S1dsDNA1.154) particles when incubated with 20 μM hairpins (Supp. Fig. 8b). This observation leads to an intriguing hypothesis about whether the R connection is necessary for swelling. In another experiment depicted in Supplementary Figure 9, we compared the swelling of different poly(Am-co-DNA) hydrogels in response to S1 hairpins. All hydrogels contained dsDNA that is conjugated to the polymer backbone on both strands. The first type of hydrogel had S1 dsDNA conjugated by both ends whereas the second group had S3 dsDNA conjugated by both ends. The second group of hydrogels also had S1 dsDNA that is only conjugated to the polymer backbone by the A strand side. When adding S1 hairpins to these two groups of hydrogels, we would therefore expect that both would swell and that the first group would swell by extension of mechanically coupled crosslinks, whereas the second would swell via polymer extension through a simple polyelectrolyte effect. If the R connection is unimportant, we would expect the swelling to be the same. However, Supp. Fig. 9 shows the gels with the doubly conjugated S1 dsDNA exhibit 4 times greater swelling on average than the gels with the dsDNA conjugated only to the A strand. It, therefore, appears we need to better understand the role of the R connection and R strand in different materials and contexts. Another potential factor in the R connection is that DNA crosslinks in a gel contribute to the mechanical modulus. We previously demonstrated that the presence of dsDNA crosslinks can significantly increase a hydrogel's modulus by 20-45%.<sup>23</sup> If the gel's swelling was entirely a polyelectrolyte effect, then the use of the dsDNA as a crosslink should actually slightly inhibit swelling as compared to the inclusion of the dsDNA conjugated by only one strand.

#### **Conclusions and outlook**

Here, we have investigated how altering features of the DNA crosslinks and hairpins that control the kinetics and degree of DNA strand displacement, in turn, affect the rate and extent of DNA polymerization gel swelling.

While none of the parameters we tested induced order-of-magnitude or greater changes in the rate of hydrogel swelling, we identified design parameters with the strongest effects on swelling rates and extent. Of note, the concentration of anchored DNA inside hydrogels had the greatest effect on both the kinetics and degree of swelling. Next in importance was the concentration of hairpin fuel used to swell the gels and its effect was dependent on the sequences. The lengths of the toeholds were found to be the least important factor.

We also showed that hydrogels could be expanded using the HCR process by integrating single-stranded DNA initiators or single side-anchored dsDNA into the hydrogel matrix. Using these types of initiators decreases the number of acrydite-modified DNA strands by half, reducing the DNA-responsive hydrogel device production cost.

When we varied the gel thicknesses (60  $\mu$ m or 160  $\mu$ m), we discovered that these factors have limited effects on the swelling process. Larger gel dimensions (e.g., a 320  $\mu$ m thickness) or different gel shapes (sheets or sphere-like particles) that limit diffusion can largely decrease the gel swelling.

Finally, it is the DNA polymerization at DNA crosslinks that drives the swelling of DNA polymerization gels. The swelling process involves the transport of water and ions and the reorganization of the polymer network. In future studies, the ability to choose the physical properties of the gel (e.g., diffusion coefficients of different molecules, locking stretch, and Flory-Huggins interaction parameter) could help us develop a design strategy that considers the combined thermodynamic and kinetic effects to allow for the rational design of such responsive polymerization gels.

#### Conflicts of interest

There are no conflicts to declare.

### Acknowledgements

The authors gratefully acknowledge DOE Early Career Award BES 221874 to R.Sc., a JHU Catalyst Award to R.Sc., and the NSF EFMA Award 1830893 to D.H.G. and R.Sc. for support of this work.

This work was also sponsored by the Army Research Office and was accomplished under Cooperative Agreement Number W911NF-22-2-0246 to R.Sc.. The views and conclusions contained in this document are those of the authors and should not be interpreted as representing the official policies, either expressed or implied, of the Army Research Office or the U.S. Government. The U.S. Government is authorized to reproduce and distribute reprints for Government purposes notwithstanding any copyright notation herein.

#### **Notes and references**

- X. Liu, J. Liu, S. Lin and X. Zhao, *Mater. Today*, 2020, 36, 102–124.
- 2 J. Tavakoli and Y. Tang, *Polymers (Basel).*, 2017, **9**, 1–25.
- N. A. Peppas, J. Z. Hilt, A. Khademhosseini and R. Langer, *Adv. Mater.*, 2006, 18, 1345–1360.
- 4 I. Apsite, S. Salehi and L. Ionov, *Chem. Rev.*, 2022, **122**, 1349–1415.
- 5 M. Vázquez-González and I. Willner, *Angew. Chemie Int. Ed.*, 2020, **59**, 15342–15377.
- O. Erol, A. Pantula, W. Liu and D. H. Gracias, *Adv. Mater. Technol.*, 2019, 4, 1900043.
- 7 M. C. Koetting, J. T. Peters, S. D. Steichen and N. A. Peppas, *Mater. Sci. Eng. R Reports*, 2015, **93**, 1–49.
- J. Leijten, J. Seo, K. Yue, G. T. Santiago, A. Tamayol, G. U. Ruiz-esparza, S. R. Shin, R. Sharifi, I. Noshadi, M. M. Álvarez, Y. S. Zhang and A. Khademhosseini, *Mater. Sci. Eng. R*, 2017, 119, 1–35.
- 9 G. Sharifzadeh and H. Hosseinkhani, *Adv. Healthc. Mater.*, 2017, **6**, 1700801.
- M. Moshinsky, Biomedical Applications of Hydrogels Handbook, Springer New York, New York, NY, 2010, vol. 13.
- J. Hoque, N. Sangaj and S. Varghese, *Macromol. Biosci.*, 2019, 19, 1800259.

Journal Name ARTICLE

- 12 L. Klouda and A. G. Mikos, *Eur. J. Pharm. Biopharm.*, 2008, **68**, 34–45.
- M. Abdul, Y. Su and D. Wang, *Mater. Sci. Eng. C*, 2017, **70**, 842–855.
- 14 Y. Dong, A. N. Ramey-Ward and K. Salaita, *Adv. Mater.*, 2021, **33**, 2006600.
- 15 Y. Guan and Y. Zhang, *Soft Matter*, 2011, 7, 6375–6384.
- D. Wang, Y. Hu, P. Liu and D. Luo, *Acc. Chem. Res.*, 2017, 50, 733–739.
- N. Xu, N. Ma, X. Yang, G. Ling, J. Yu and P. Zhang, *Eur. Polym. J.*, 2020, **137**, 109951.
- F. Li, D. Lyu, S. Liu and W. Guo, Adv. Mater., 2020, 32, 1806538.
- J. S. Kahn, Y. Hu and I. Willner, Acc. Chem. Res., 2017, 50, 680–690.
- 20 X. Xiong, C. Wu, C. Zhou, G. Zhu, Z. Chen and W. Tan, Macromol. Rapid Commun., 2013, 34, 1271–1283.
- 21 F. Mo, K. Jiang, D. Zhao, Y. Wang, J. Song and W. Tan, *Adv. Drug Deliv. Rev.*, 2021, **168**, 79–98.
- A. Cangialosi, C. Yoon, J. Liu, Q. Huang, J. Guo, T. D. Nguyen, D. H. Gracias and R. Schulman, *Science*, 2017, **357**, 1126–1130.
- 23 R. Shi, J. Fern, W. Xu, S. Jia, Q. Huang, G. Pahapale, R. Schulman and D. H. Gracias, *Small*, 2020, **16**, 2002946.
- 24 J. Fern and R. Schulman, *Nat. Commun.*, 2018, **9**, 1–8.
- 25 R. Shi, K.-L. Chen, J. Fern, S. Deng, Y. Liu, D. Scalise, Q. Huang, N. J. Cowan, D. H. Gracias and R. Schulman, *bioRxiv*, 2022, 2022.09.21.508918.
- S. Venkataraman, R. M. Dirks, P. W. K. Rothemund, E. Winfree and N. A. Pierce, *Nat. Nanotechnol.*, 2007, **2**, 490–494.
- N. L. Dabby, Dissertation, California Institute of Technology, 2013.
- D. Y. Zhang and E. Winfree, J. Am. Chem. Soc., 2009, 131, 17303–17314.
- 29 R. M. Dirks and N. A. Pierce, *Proc. Natl. Acad. Sci.*, 2004, **101**, 15275–15278.
- 30 R. Owczarzy, B. G. Moreira, Y. You, M. A. Behlke and J. A. Walder, *Biochemistry*, 2008, **47**, 5336–5353.
- J. H. Espenson, *Chemical kinetics and reaction mechanisms*, McGraw-Hill, Inc., New York, Second Edi., 1995.
- N. Srinivas, T. E. Ouldridge, P. Sulc, J. M. Schaeffer, B. Yurke, A. A. Louis, J. P. K. Doye and E. Winfree, *Nucleic Acids Res.*, 2013, **41**, 10641–10658.
- 33 W. F. Dove and N. Davidson, *J. Mol. Biol.*, 1962, **5**, 467–478.
- 34 M. Shibayama and T. Tanaka, in *Advances in Polymer Science*, 1993, vol. 109, pp. 1–62.
- 35 J. R. Choi, K. W. Yong, J. Y. Choi and A. C. Cowie, *Biotechniques*, 2019, **66**, 40–53.
- 36 Y. S. Ang and L.-Y. L. Yung, *Chem. Commun.*, 2016, **52**, 4219–4222.
- B. Groves, Y. Chen, C. Zurla, S. Pochekailov, J. L. Kirschman,
   P. J. Santangelo and G. Seelig, *Nat. Nanotechnol.*, 2016, 11,
   287–294.
- 38 S. Ghosh, S. Takahashi, T. Endoh, H. Tateishi-karimata, S. Hazra and N. Sugimoto, *Nucleic Acids Res.*, 2019, **47**, 3284–3294.

- 39 J. SantaLucia, *Proc. Natl. Acad. Sci.*, 1998, **95**, 1460–1465.
- J. M. Huguet, M. Ribezzi-crivellari, C. V. Bizarro and F. Ritort, *Nucleic Acids Res.*, 2017, **45**, 12921–12931.
- W. M. Deen, *Analysis of Transport Phenomena*, Oxford University Press, 1998.

# **Supplementary Information for**

# Swelling characteristics of DNA polymerization gels

Joshua Fern, † Ruohong Shi, † Yixin Liu, a Yan Xiong, a David H. Gracias \* a - g and Rebecca Schulman \* abgh

<sup>&</sup>lt;sup>a</sup> Department of Chemical and Biomolecular Engineering, Johns Hopkins University, Baltimore, MD 21218, United States of America;

<sup>&</sup>lt;sup>b</sup> Laboratory for Computational Sensing and Robotics (LCSR), Johns Hopkins University, Baltimore, MD 21218, United States of America;

<sup>&</sup>lt;sup>c</sup> Center for MicroPhysiological Systems (MPS), Johns Hopkins University, Baltimore, MD 21218, United States of America;

<sup>&</sup>lt;sup>d</sup> Department of Oncology, Johns Hopkins School of Medicine, Baltimore, MD 21218, United States of America;

<sup>&</sup>lt;sup>e</sup> Sidney Kimmel Comprehensive Cancer Center (SKCCC), Johns Hopkins School of Medicine, Baltimore, MD 21218, United States of America;

<sup>&</sup>lt;sup>f</sup> Department of Materials Science and Engineering, Johns Hopkins University, Baltimore, MD 21218, United States of America;

<sup>&</sup>lt;sup>9</sup> Department of Chemistry, Johns Hopkins University, Baltimore, MD 21218, United States of America;

<sup>&</sup>lt;sup>h</sup> Computer Science, Johns Hopkins University, Baltimore, MD 21218, United States of America.

<sup>†</sup> Equal contribution.

<sup>\*</sup> Corresponding author. Email: rschulm3@jhu.edu; dgracias@jhu.edu.

### **Materials and Methods**

#### **Chemicals and DNA**

Polyethylene glycol diacrylate M<sub>n</sub> 10,000 (PEGDA10k) was obtained from Sigma-Aldrich (Cat. No. 729094). The fluorophore RhodamineB-methacrylate was purchased from PolySciences, Inc. (Cat. No. 25404-100) and was used to visualize the hydrogels. Acrylamide (Bio-Rad, Cat. No. 161-0100) was solubilized in MilliQ purified water. The UV-sensitive initiator Omnirad 2100 (formerly known as Irgacure 2100, iGM Resins USA, #55924582) photoinitiator was used to polymerize hydrogels. All DNA strands were purchased with standard desalting purification from Integrated DNA Technologies, Inc. Acrydite-modified strands were solubilized using 1x TAE buffer (Life Technologies, Cat. No. 24710-030) supplemented with 12.5 mM magnesium acetate tetrahydrate (Sigma-Aldrich, Cat. No. M5661). All unmodified DNA strands were solubilized using MilliQ purified water. DNA sequences were adapted from previous literature<sup>1–3</sup> or designed using NUPACK<sup>4</sup> as previously described<sup>2</sup> and are listed in Supplementary Table 1.

#### **Preparation of DNA complexes**

DNA crosslink complexes were annealed in 1x TAE buffer supplemented with 12.5 mM magnesium acetate tetrahydrate (TAEM) from 90 to 20 °C in an Eppendorf PCR at 1 °C/minute at a concentration of 3 mM per strand. Hairpin-forming strands were heated to 95 °C for 15 minutes at a concentration of 200 or 600  $\mu$ M, followed by flash cooling on ice for 3 minutes.

#### Preparation of poly(PEGDA10k-co-DNA) pre-gel solution

PEGDA10k powder was mixed with MilliQ purified water and 10x TAEM. After the PEGDA10k was fully dissolved, acrydite-modified DNA (3 mM), RhodamineB-methacrylate (29.9 mM), and Omnirad 2100 (75% v/v in butanol) were mixed into the solution. The final

concentrations were 10% w/v PEGDA10k, 2.74 mM RhodamineB, and 3% v/v Irgacure 2100. Unless noted otherwise, the final concentration of DNA strands or complexes was 1.154 mM. After mixing with a pipette, the pre-gel solution was sonicated for 10 minutes and degassed for 15 minutes.

#### Synthesis of poly(PEGDA10k-co-DNA) hydrogel triangles

We assembled photolithography chambers, as reported previously.<sup>1,5</sup> To pattern equilateral triangle-shaped DNA hydrogels, we designed triangle-shaped masks with 1mm sidelength using AutoCAD and made the Cr masks using the method reported.<sup>1,5</sup> The thickness of the patterned hydrogel could be tuned using different thicknesses of spacers (160 µm in this paper unless otherwise stated). The pre-gel solution was injected into the photo patterning chamber and then exposed to a 365 nm UV light source (Neutronix Quintel aligner) with an energy dose of 600 mJ/cm<sup>2</sup>. The chamber was gently disassembled after the polymerization. We use TAEM to wash the extra pre-gel solution and hydrate the gel. The hydrogel was then stored in the TAEM at 4 °C to achieve complete hydration until use; the portion of intrinsic swelling with TAEM was not included in the swelling kinetics calculations.

### Preparation of poly(Am-co-DNA) pre-gel solution

Acrylamide, acrydite-modified DNA (3 mM), RhodamineB-methacrylate (29.9 mM), and Irgacure 2100 (75% v/v in butanol) were mixed into the solution. The final concentrations were 10% w/v PEGDA10k, 2.74 mM RhodamineB, and 3% v/v Irgacure 2100. The final concentration of DNA strands or complexes was 1.154 mM unless noted otherwise. After mixing with a pipette, the pre-gel solution was sonicated for 10 minutes and degassed for 15 minutes.

#### Synthesis of hydrogel particles

DNA-integrated polyacrylamide and PEGDA10k hydrogel particles were prepared as previously described.<sup>2</sup> Hydrogel droplets were polymerized in mineral oil with 365 nm light using a Benchtop 3UV Transilluminator (UVP) for 1.5 minutes. Polymerized particles were purified from the mineral oil and stored in 1x TAEM at room temperature or 4°C until use.

#### **Swelling DNA-integrated hydrogels**

Hydrogel swelling experiments were conducted with one hydrogel per well in 96-well plates (Fisher Scientific). Unless noted otherwise, hydrogels were expanded in TAEM supplemented with 0.001% v/v Tween20 to prevent hydrogel from sticking to the well's surface. Hairpins were added such that at least 60  $\mu$ L of the 100  $\mu$ L total in each well was TAEM with Tween20, and the remaining solution was the hairpin stock solution. Following the addition of hairpin solutions to each well, we utilized a pipette set to a volume of 90  $\mu$ L and thoroughly mixed the solution by performing at least 10 times repeatedly dispensing and withdrawing. Images were captured every 30 minutes using a humidified Syngene G:Box EF2 gel imager equipped with a blue light transilluminator (Clare Chemical, Em. max ~450 nm) and a UV032 filter (Syngene, bandpass 572-630 nm) or on an Olympus IX73 fluorescence microscope.

#### Experiments comparing hydrogel expansion in different buffer/salt conditions

Hydrogel swelling experiments were conducted with one hydrogel per well in 96-well plates (Fisher Scientific). The volume of liquid in each well was 100  $\mu$ L. The stock concentrations of buffers were 5x for SPSC and 10x for PBS, TAE/Mg<sup>2+</sup>, TAE/Na<sup>+</sup>, and TAE/Mg<sup>2+</sup>/Na<sup>+</sup>. The concentrations of species in each 1x buffer are listed in Supp. Table 2.

For poly(Am-co-S1dsA<sup>ac</sup>R<sup>ac</sup>1.154) hydrogel particles, the hairpin stock solutions were at 400  $\mu$ M per hairpin and were snap cooled in 1x TAEM. The hairpin concentration during hydrogel

expansion was initially 20  $\mu$ M per hairpin. The reaction volume for 10x buffers consisted of 10  $\mu$ L of 10x buffer, 80  $\mu$ L MilliQ water, and 5  $\mu$ L each hairpin stock solution. The reaction volume for 5x buffers consisted of 20  $\mu$ L of 5x buffer, 70  $\mu$ L MilliQ water, and 5  $\mu$ L each hairpin stock solution. Since the hairpins were snap cooled in 1x TAEM, the final buffer conditions in each condition included an additional 0.1x TAEM (*e.g.*, "TAE/Mg<sup>2+</sup>" had 1.1x TAEM buffer, "PBS" had 1x PBS + 0.1x TAEM). The salt concentrations for expanding poly(Am-*co*-S1dsA<sup>ac</sup>R<sup>ac</sup>1.154) hydrogel particles in varying buffers are listed in Supp. Table 3.

For poly(PEGDA10k-co-S1dsAacRac1.154) hydrogel triangle and particles, the hairpin stock solutions were at 200  $\mu$ M per hairpin and were snap cooled in 1x TAEM. The hairpin concentration during hydrogel expansion was initially 20  $\mu$ M per hairpin. The reaction volume for 10x buffers consisted of 10  $\mu$ L of 10x buffer, 70  $\mu$ L MilliQ water, and 10  $\mu$ L each hairpin stock solution. The reaction volume for 5x buffers consisted of 20  $\mu$ L of 5x buffer, 60  $\mu$ L MilliQ water, and 10  $\mu$ L each hairpin stock solution. Since the hairpins were snap cooled in 1x TAEM, the final buffer conditions in each condition included an additional 0.2x TAEM (e.g., "TAE/Mg²+" had 1.2x TAEM buffer, "PBS" had 1x PBS + 0.2x TAEM). The salt concentrations for expanding poly(PEGDA10k-co-S1dsAacRac1.154) hydrogel triangles and particles in varying buffers are listed in Supp. Table 4.

Images were captured every 30 minutes using a humidified Syngene G:Box EF2 gel imager equipped with a blue light transilluminator (Clare Chemical, Em. max  $^{\sim}450$  nm) and a UV032 filter (Syngene, bandpass 572-630 nm) or on an Olympus IX73 fluorescence microscope. The equivalent Na $^{+}$  concentration in Supp. Tables 3 and 4 were calculated using equation 0 from Owczarzy *et al.*<sup>6</sup> The value of  $\beta$  was chosen to be 3.75, a value in the middle of the range of expected values for  $\beta$ .

$$[Na^{+}]_{eq} = [Monovalent\ Cations] + \beta \sqrt{[Divalent\ Cations]}$$
 (0)

### Analysis of hydrogel triangle swelling

The relative change in the side length of the hydrogels was measured using MATLAB. The edge of the hydrogel was determined using standard intensity-based thresholding and mask image analysis. First, the intensity values of the image were globally adjusted using *imadjust* to saturate the bottom and top 1% of all pixel values. A Gaussian low-pass filter was applied to this adjusted image to reduce or remove background noise and generate the filtered image (FiltImg). The filtered image was then rotated so that the edges of the hydrogel triangle were not perfectly horizontal or vertical to aid in vertex detection.

A two-step process was used to determine the threshold used to find the hydrogel's edges.

A general mask was generated from the filtered image using the following:

$$GenMask = FiltImg \ge 1.35 * mean(FiltImg)$$
 (1)

The general mask (GenMask) is a logical matrix where values of one indicate the bulk hydrogel plus some extra background pixels. The threshold value was then calculated using equation 4.

$$PixOne\ matrix = FiltImg\ pixel\ values\ where\ GenMask\ pixels\ are\ 1$$
 (2)

$$PixZero\ matrix = FiltImg\ pixel\ values\ where\ GenMask\ pixels\ are\ 0$$
 (3)

$$Thresh = \frac{mean(PixOne)}{mean(PixZero) * \alpha}$$
 (4)

The parameter alpha varied from image to image in order to provide a good agreement between the calculated boundary and the observed boundary of the hydrogel. The matrix PixZero generally represents the background pixels of the image. The final mask, with values of one indicating the pixels belonging to the hydrogel object (at least), was calculated using the threshold (Thresh) in equation 4:

$$HydMask = FiltImg \ge Thresh * mean(FiltImg)$$
 (5)

Objects were removed (values set to 0) from HydMask if their total area was less than 700 pixels. The area of the hydrogels was at least 800 pixels in size. The boundary of the hydrogel was determined using MATLAB's *bwboundaries* function using a connectivity of 8.

The vertices of the hydrogel were determined from the extrema of the hydrogel object. The extrema and centroids of the objects in HydMask were determined using MATLAB's function regionprops. If background objects (e.g., the side of the well) were found in HydMask, the object with a centroid closest to the center of the image was chosen to be the hydrogel object. k-means clustering was used to determine the location of the vertices from the 8 locations provided by the extrema of the hydrogel object. The algorithm was set to detect 4 clusters, and the 3 clusters that were the farthest apart were the vertices of the hydrogel. The average distance between these three clusters was used as the measure of the side length of the hydrogel. The relative change in the side length of the hydrogel was calculated using the measured side length (L) for each image in a time series relative to the side length prior to adding hairpins (L<sub>0</sub>).

$$\frac{\Delta L}{L_0} = \frac{L - L_0}{L_0} \tag{6}$$

For each treatment variable plotted in the figures, the average relative change in side length  $(\bar{x})$  was calculated by taking the mean value of at least three hydrogel swelling time series curves (n measurements). The 95% confidence interval bounds for each average measurement were calculated by calculating the standard deviation (s) of the swelling curves and multiplying by the 95<sup>th</sup> percentile of the Student's t distribution for n-1 degrees of freedom:

$$Bounds = \bar{x} \pm t \cdot \frac{s}{\sqrt{n}} \tag{7}$$

where t is calculated using MATLAB's tinv function.

# Analysis of hydrogel particle swelling

Hydrogel particles were analyzed using MATLAB as previously described.<sup>2</sup> First, the area of the hydrogel particle was calculated from the number of pixels within the boundary of the particle in the micrograph. Next, the area (A) was converted into the radius (r) of the particle using:

$$r = \sqrt{A\pi} \tag{8}$$

The change in the radius, relative to the radius in the first image of the time series immediately after adding hairpins, was calculated using:

$$\frac{\Delta r}{r_0} = \frac{r - r_0}{r_0} \tag{9}$$

**Supplementary Table 1**: List of DNA sequences. Sequences were taken from previous literature<sup>1,7</sup> or designed using NUPACK.<sup>4</sup> Each hairpin's toehold lengths are listed as "primary toehold/secondary toehold" after the period in the strand name and in the role columns.

Strand Name	Role	Sequence					
Crosslinks							
A_S1 (A1_a6)	Sequence set 1, 6bases primary toehold	/5Acryd/TAAGTT CGCTGTGGCACCTGCACG					
R_S1 (R1_x3y3)	Sequence set 1, 3bases secondary toeholds	/5Acryd/CAA CGTGCAGGTGCCACAGCG TGG					
A_S2 (A5_a10)	Sequence set 2 v1 & v2, 10bases primary toehold	/5Acryd/CTCTATCTAT CCATCACCCTCACCTTAC					
A_S2a6 (A5_a6)	Sequence set 2 v3, 6bases primary toehold	/5Acryd/ATCTAT CCATCACCCTCACCTTAC					
R_S2 (R5_x3y3)	Sequence set 2 v1 & v3, 3bases secondary toeholds	/5Acryd/GGT GTAAGGTGAGGGTGATGG TAA					
R_S2x6 (R5_x6y6)	Sequence set 2 v2, 6bases secondary toeholds	/5Acryd/TGAGGT GTAAGGTGAGGGTGATGG TAAAGG					
A_S3 (A2_a6)	Sequence set 3, 6bases primary toeholds	/5Acryd/CTGTCT GCCTACCACTCCGTTGCG					
R_S3 (R2_x3y3)	Sequence set 3, 3bases secondary toeholds	/5Acryd/ATT CGCAACGGAGTGGTAGGC TTT					
	Hairpin Stra	nds					
H1 S1 6/3	Hairpin monomer, sequence set 1, 6/3bases	CCA CGCTGTGGCACCTGCACG CACCCA					
(H1_s1.6/3)	toeholds	CGTGCAGGTGCCACAGCG AACTTA					
H2_S1_6/3	Hairpin monomer, sequence set 1, 6/3bases	TGGGTG CGTGCAGGTGCCACAGCG TAAGTT					
(H2_s1.6/3)	toeholds	CGCTGTGGCACCTGCACG TTG					
H1_S2_10/3	Hairpin monomer, sequence set 2,	TTA CCATCACCCTCACCTTAC TTGTAGATTG					
(H1_s5.10/3)	10/3bases toeholds	GTAAGGTGAGGGTGATGG ATAGATAGAG					
H2_S2_10/3	Hairpin monomer, sequence set 2,	CAATCTACAA GTAAGGTGAGGGTGATGG CTCTATCTAT					
(H2_s5.10/3)	10/3bases toeholds	CCATCACCCTCACCTTAC ACC					
H1_S2_8/3	Hairpin monomer, sequence set 2, 8/3bases	TTA CCATCACCCTCACCTTAC TTGTAGAT					
(H1_s5.8/3)	toeholds	GTAAGGTGAGGGTGATGG ATAGATAG					
H2_S2_8/3	Hairpin monomer, sequence set 2, 8/3bases	ATCTACAA GTAAGGTGAGGGTGATGG CTATCTAT					
(H2_s5.8/3)	toeholds	CCATCACCCTCACCTTAC ACC					
H1_S2_6/3	Hairpin monomer, sequence set 2, 6/3bases	TTA CCATCACCCTCACCTTAC TTGTAG					
(H1_s5.6/3)	toeholds	GTAAGGTGAGGGTGATGG ATAGAT					
H2_S2_6/3	Hairpin monomer, sequence set 2, 6/3bases	CTACAA GTAAGGTGAGGGTGATGG ATCTAT					
(H2_s5.6/3)	toeholds	CCATCACCCTCACCTTAC ACC					
H1_S2_8/6	Hairpin monomer, sequence set 2, 8/6bases	CCTTTA CCATCACCCTCACCTTAC ACC					
(H1_s5.8/6)	toeholds	GTAAGGTGAGGGTGATGG ATAGATAG					
H2_S2_8/6	Hairpin monomer, sequence set 2, 8/6bases	ATCTACAA GTAAGGTGAGGGTGATGG CTATCTAT					
(H2_s5.8/6)	toeholds	CCATCACCTCACCTTAC ACCTCA					
H1 S2 6/6	Hairpin monomer, sequence set 2, 6/6bases	CCTTTA CCATCACCTTAC ACCTCA  CCTTTA CCATCACCCTCACCTTAC TTGTAG					
(H1_s5.6/6)	toeholds	GTAAGGTGAGGGTGATGG ATAGAT					
H2_S2_6/6	Hairpin monomer, sequence set 2, 6/6bases	CTACAA GTAAGGTGAGGGTGATGG ATCTAT					
(H2_s5.6/6)	toeholds	CCATCACCTCACCTTAC ACCTCA					
H1 S3 6/3	Hairpin monomer, sequence set 3, 6/3bases	AAA GCCTACCACTCCGTTGCG GAACCT					
(H1_s2.6/3)	toeholds	CGCAACGGAGTGGTAGGC AGACAG					
H2_S3_6/3	Hairpin monomer, sequence set 3, 6/3bases	AGGTTC CGCAACGGAGTGGTAGGC CTGTCT					
(H2_s2.6/3)	toeholds	GCCTACCACTCCGTTGCG AAT					
H1_S1_ter	Terminator hairpin monomer, sequence set	CCA CGCTGTGGCACCTGCACG TAGACT					
(H1_s1.ter)	1, 6/3bases toeholds	CGTGCAGGTGCCACAGCG AACTTA					
H2 S1 ter	Terminator hairpin monomer, sequence set	TGGGTG CGTGCAGGTGCCACAGCG GCCTAG					
(H2_s1.ter)	1, 6/3bases toeholds	CGCTGTGGCACCTGCACG TTG					
	Hairpin monomer, sequence set 2, used in	TTACCATCACCCTCACCTTACTTGTAGATTTTTTGTAAGGTGA					
H1_S2_mb	mass balance studies	GGGTGATGGATAGATAGGGTAGGTGAATGGGA					

H2_S2_mb	Hairpin monomer, sequence set 2, used in	TATGAGTGAGTTAGGATCTACAAGTAAGGTGAGGGTGATGG		
	mass balance studies	TTTTTCTATCTATCCATCACCCTCACCTTACACC		
H1_S2_mb_ter	Terminator hairpin monomer, sequence set	TTACCATCACCCTCACCTTACCTCTCCACTTTTTGTAAGGTGA		
	2, used in mass balance studies	GGGTGATGGATAGATAGGGTAGGTGAATGGGA		
U2 C2 mb tor	Terminator hairpin monomer, sequence set	TATGAGTGAGTTAGGATCTACAAGTAAGGTGAGGGTGATGG		
H2_S2_mb_ter	4, used in mass balance studies	TTTTTACGAGCCTCCATCACCCTCACCTTACACC		
H1_S4_mb	Hairpin monomer, sequence set 4, used in	ATCCCACTCACACTCCACTCCCGCTCGCCTAATAGGAGTGGA		
	mass balance studies	GTGTGAGTGGAGTGGTAGGTTAGGTGAGGTGG		
H2_S4_mb	Hairpin monomer, sequence set 4, used in	GTTGTAAGTGAGAGTGGCGAGCGGGAGTGGAGTGTGAGT		
	mass balance studies	GGTAATACTACCACTCCACTCACACTCCACTCCACC		
H1_S4_mb_ter	Terminator hairpin monomer, sequence set	ATCCCACTCACACTCCACTCCGTGCTGGTTAATAGGAGTGG		
	4, used in mass balance studies	AGTGTGAGTGGAGTGGTAGGTTAGGTGAGGTGG		
H2_S4_mb_ter	Terminator hairpin monomer, sequence set	GTTGTAAGTGAGAGTGGCGAGCGGGAGTGGAGTGTGAGT		
	4, used in mass balance studies	GGTAATAAAGGCGTCCCACTCACACTCCACTCCACC		

### **Supplementary Table 2**: List of buffers and their contents.

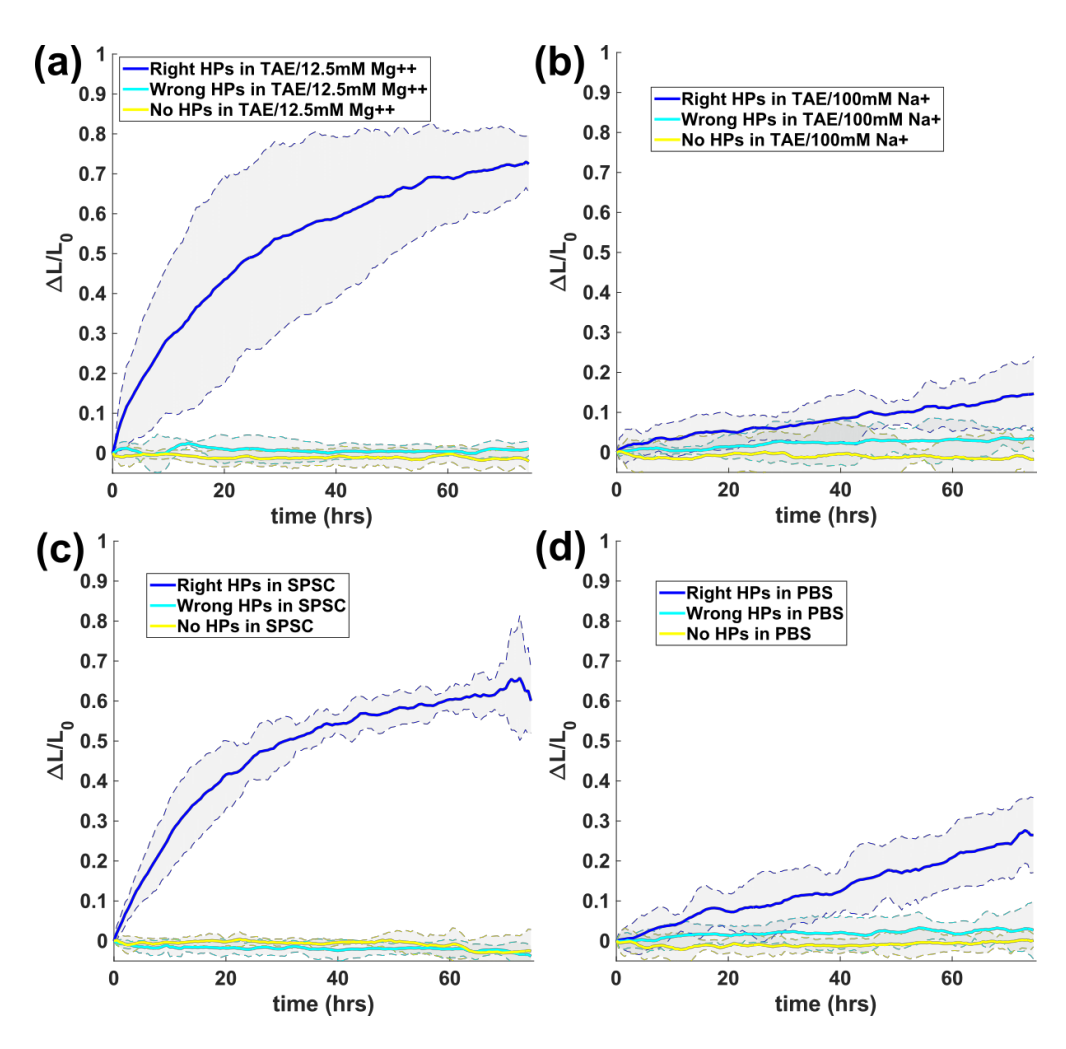
Buffer	Species			
TAE/Mg <sup>2+</sup>	40 mM Trizma, 1 mM EDTA, 20 mM Acetic Acid, 12.5 mM Mg[acetate] <sub>2</sub>			
TAE/Na <sup>+</sup>	40 mM Trizma, 1 mM EDTA, 20 mM Acetic Acid, 100 mM NaCl			
PBS	137 mM NaCl, 2.7 mM KCl, 10mM Na <sub>2</sub> HPO <sub>4</sub> , 1.8 mM KH <sub>2</sub> PO <sub>4</sub> , pH 7.4			
SPSC	1 M NaCl, 50 mM Na₂HPO₄, pH 8.0			
TAE/Mg <sup>2+</sup> /Na <sup>+</sup>	40 mM Trizma, 1 mM EDTA, 20 mM Acetic Acid, 12.5 mM Mg[acetate] <sub>2</sub> , 1 M NaCl			

**Supplementary Table 3**: Calculating the equivalent Na<sup>+</sup> concentration for each buffer used for expanding poly(Am-co-S1dsAacRac1.154) hydrogel particles (Supp. Fig. 7). The value for β was 3.75 (Equation 0).<sup>6</sup> The calculation does not take pH into account. In this case, the hairpin stock solution accounts for  $1/10^{th}$  of the total volume in the well (400 μM per hairpin stock).

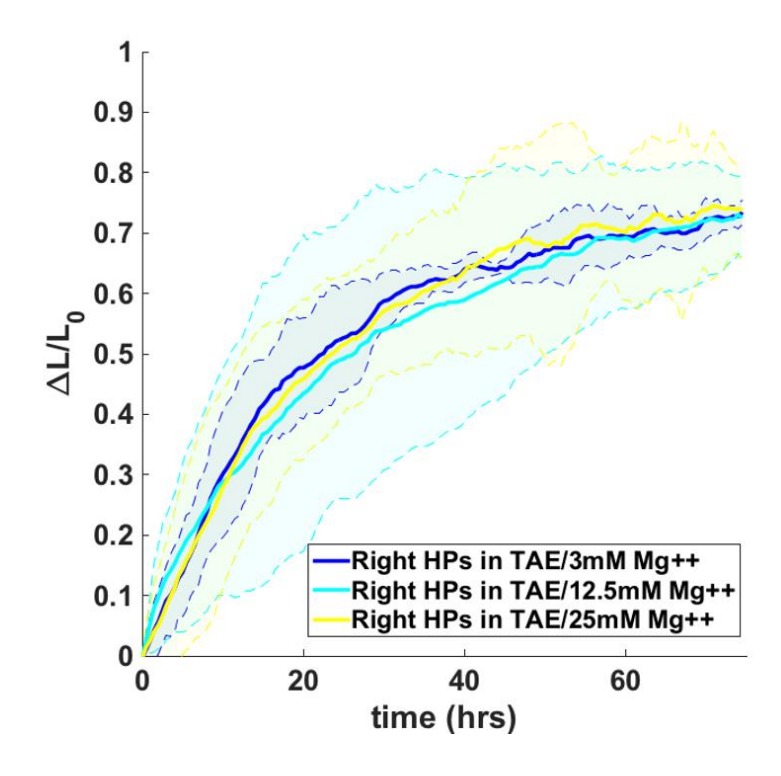
Buffer	Tris <sup>+</sup> (mM)	Na⁺ (mM)	K⁺ (mM)	Mg <sup>2+</sup> (mM)	[Mono⁺] (mM)	[Di <sup>2+</sup> ] (mM)	[Na <sup>+</sup> ] <sub>eq</sub> (mM)
TAE/Mg <sup>2+</sup>	44	0	0	13.75	44	13.75	483.73
TAE/Na⁺	44	100	0	1.25	144	1.25	276.58
PBS	4	157	4.5	1.25	165.5	1.25	298.08
SPSC	4	1100	0	1.25	1104	1.25	1236.58

**Supplementary Table 4**: Calculating the equivalent Na<sup>+</sup> concentration for each buffer used for expanding poly(PEGDA10k-co-S1dsA<sup>ac</sup>R<sup>ac</sup>1.154) hydrogel particles (Supp. Fig. 6). The value for  $\beta$  was 3.75 (Equation 0).<sup>6</sup> The calculation does not take pH into account. In this case, the hairpin stock solution accounts for  $1/5^{th}$  of the total volume in the well (200  $\mu$ M per hairpin stock).

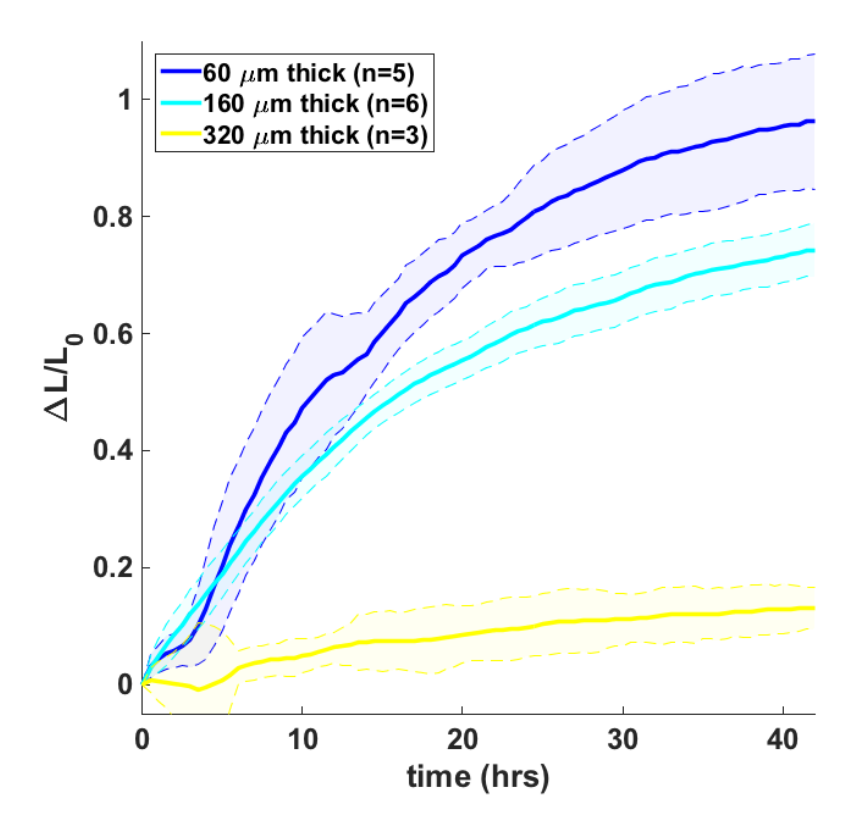
Buffer	Tris <sup>+</sup> (mM)	Na <sup>+</sup> (mM)	K <sup>+</sup> (mM)	Mg <sup>2+</sup> (mM)	[Mono <sup>+</sup> ] (mM)	[Di <sup>2+</sup> ] (mM)	[Na <sup>+</sup> ] <sub>eq</sub> (mM)
TAE/Mg <sup>2+</sup>	48	0	0	15	48	15	507.28
TAE/Na⁺	48	100	0	2.5	148	2.5	335.50
PBS	8	157	4.5	2.5	169.5	2.5	357.00
SPSC	8	1100	0	2.5	1108	2.5	1295.50
TAE/Mg <sup>2+</sup> /Na <sup>+</sup>	48	1000	0	15	1048	15	1507.28



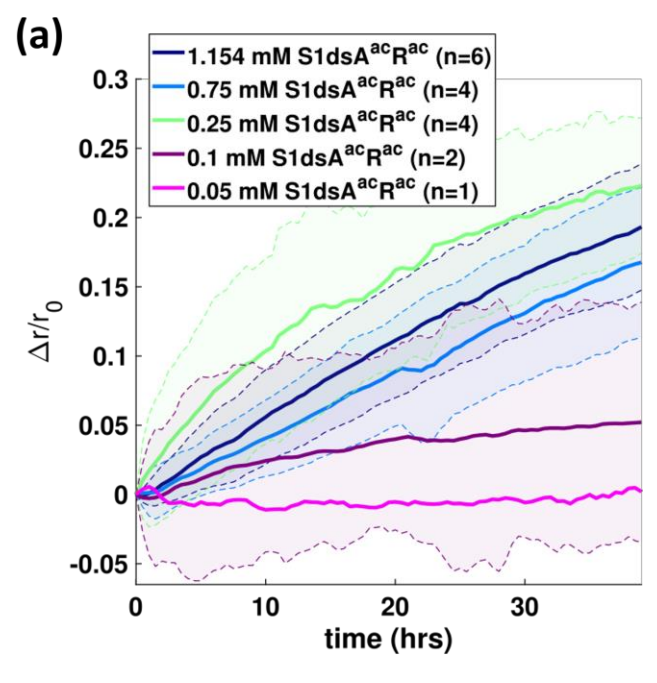
Supplementary Figure 1: The relative change in side length of poly(PEGDA10k-co-S1dsDNA1.154) hydrogels incubated with 20  $\mu$ M per hairpin with S1 HPs (H1\_S1\_6/3 and H2\_S1\_6/3, Right HPs), S3 HPs (H1\_S3\_6/3 and H2\_S3\_6/3, Wrong HPs) and buffer only (no HPs) in (a) TAE/Mg<sup>2+</sup>, (b) TAE/Na<sup>+</sup>, (c) SPSC, (d) PBS. Solid curves are the averages of measurements of the number of hydrogels shown in the legend. Shaded regions show 95% confidence intervals as determined by standard deviations. See Supp. Table 2 for buffer contents.

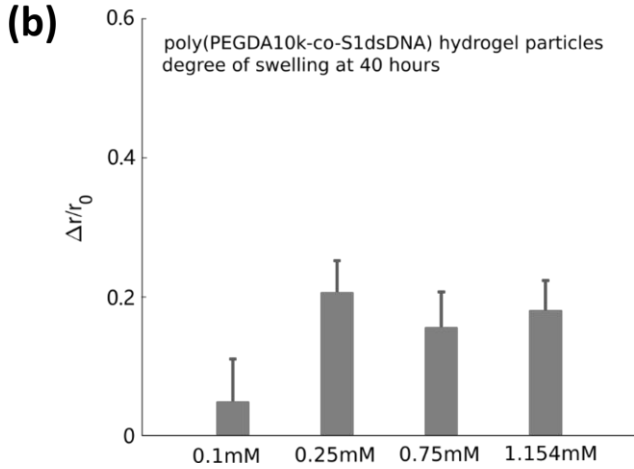


Supplementary Figure 2: The relative change in side length of poly(PEGDA10k-co-S1dsDNA1.154) hydrogel triangles incubated with 20  $\mu$ M per hairpin with S1 HPs (H1\_S1\_6/3 and H2\_S1\_6/3) in 1xTAE buffer with 3 mM, 12.5 mM, or 25 mM Mg<sup>2+</sup>. Solid curves are the averages of measurements of the number of hydrogels shown in the legend. Shaded regions show 95% confidence intervals as determined by standard deviations.

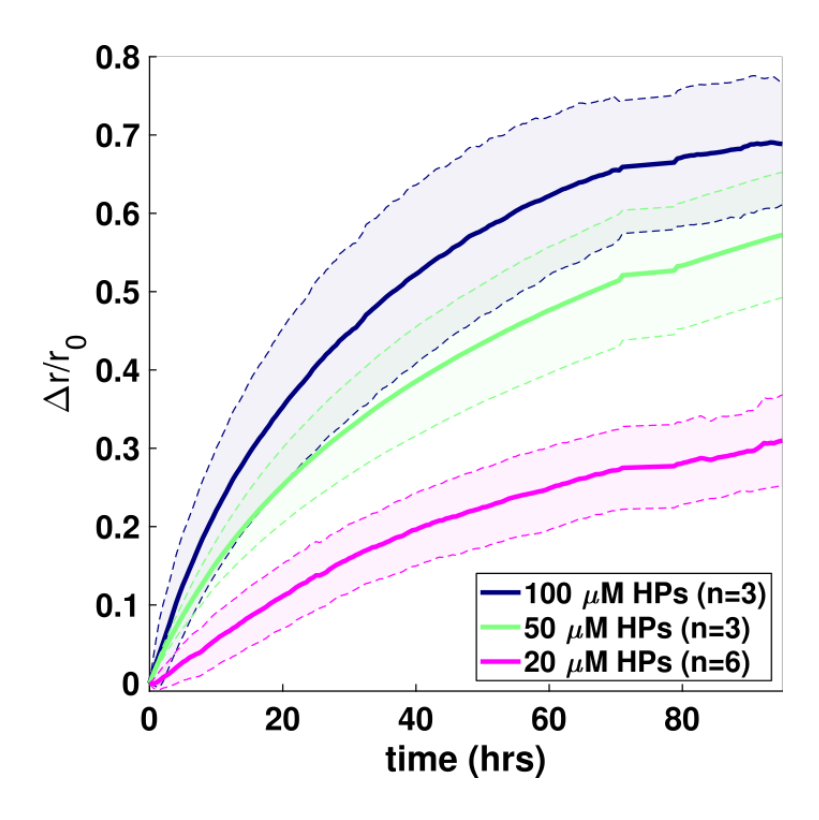


**Supplementary Figure 3**: Increasing the thickness of hydrogels reduces the extent of hydrogel expansion. The relative change in side length of poly(PEGDA10k-co-S1dsDNA1.154) hydrogels incubated with S1 HPs (H1\_S1\_6/3 and H2\_S1\_6/3) in 1x TAEM at 20  $\mu$ M per hairpin type is shown. Solid curves are the averages of measurements of the number of hydrogels shown in the legend. Shaded regions show 95% confidence intervals as determined by standard deviations.

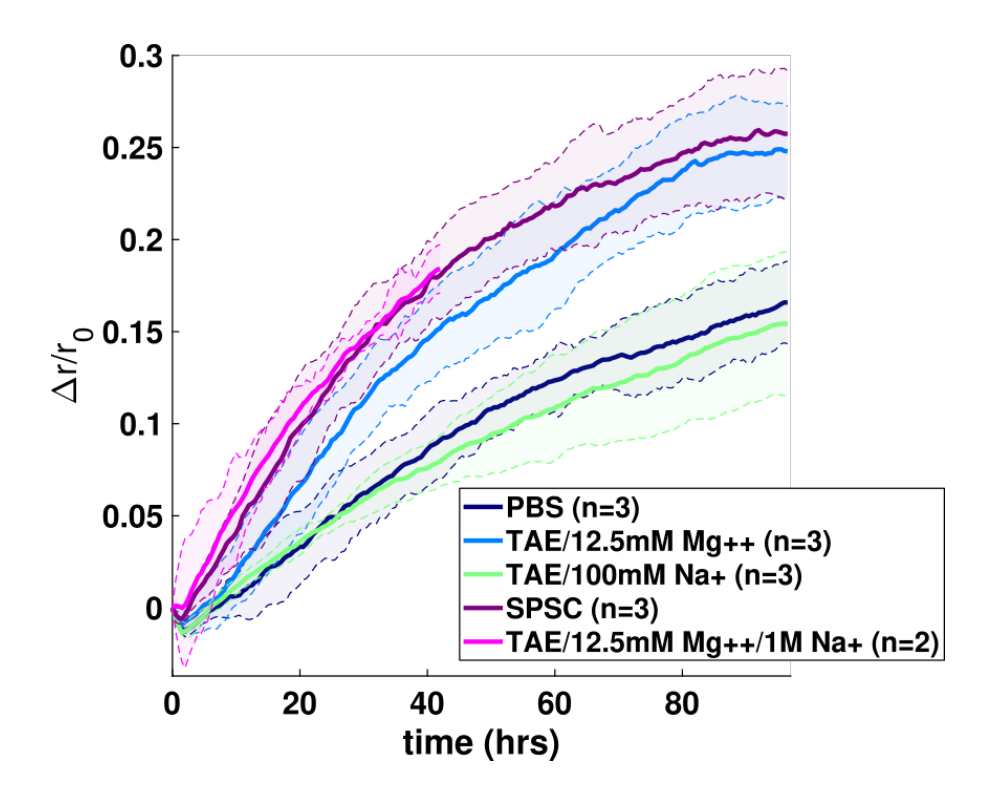




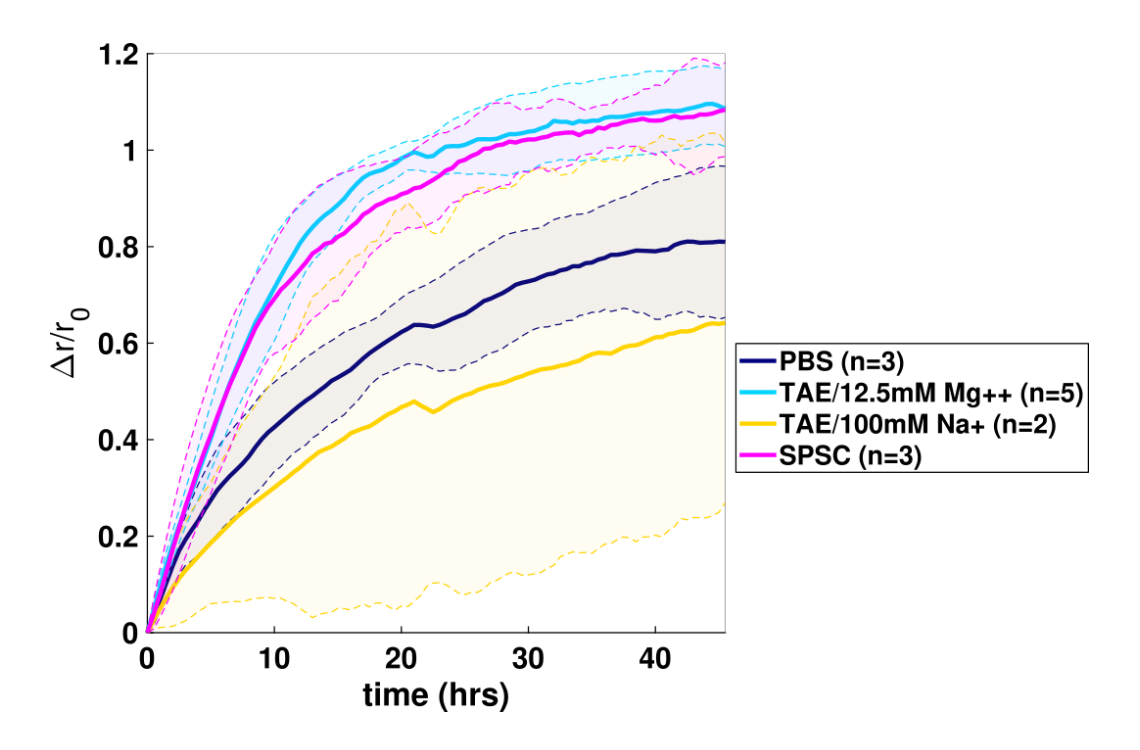
Supplementary Figure 4: (a) Relative change in average hydrogel radius of poly(PEGDA10k-co-S1dsDNA) hydrogel particles polymerized with varying concentrations of crosslinks. Sequence set 1 hairpin (H1\_S1\_6/3 and H2\_S1\_6/3) concentration was 20  $\mu$ M per hairpin in all cases. The particles were expanded in 1x TAEM. Solid curves are the averages of measurements of the number of particles shown in the legend. Shaded regions show 95% confidence intervals as determined by standard deviations. (b) Bar graph of the degree of swelling at 40 hours. In this dataset involving gel particles, the degree of swelling across the samples is consistently low and there is a significant level of sample-to-sample variance, which complicates the interpretation of results and makes it challenging to draw definitive conclusions.



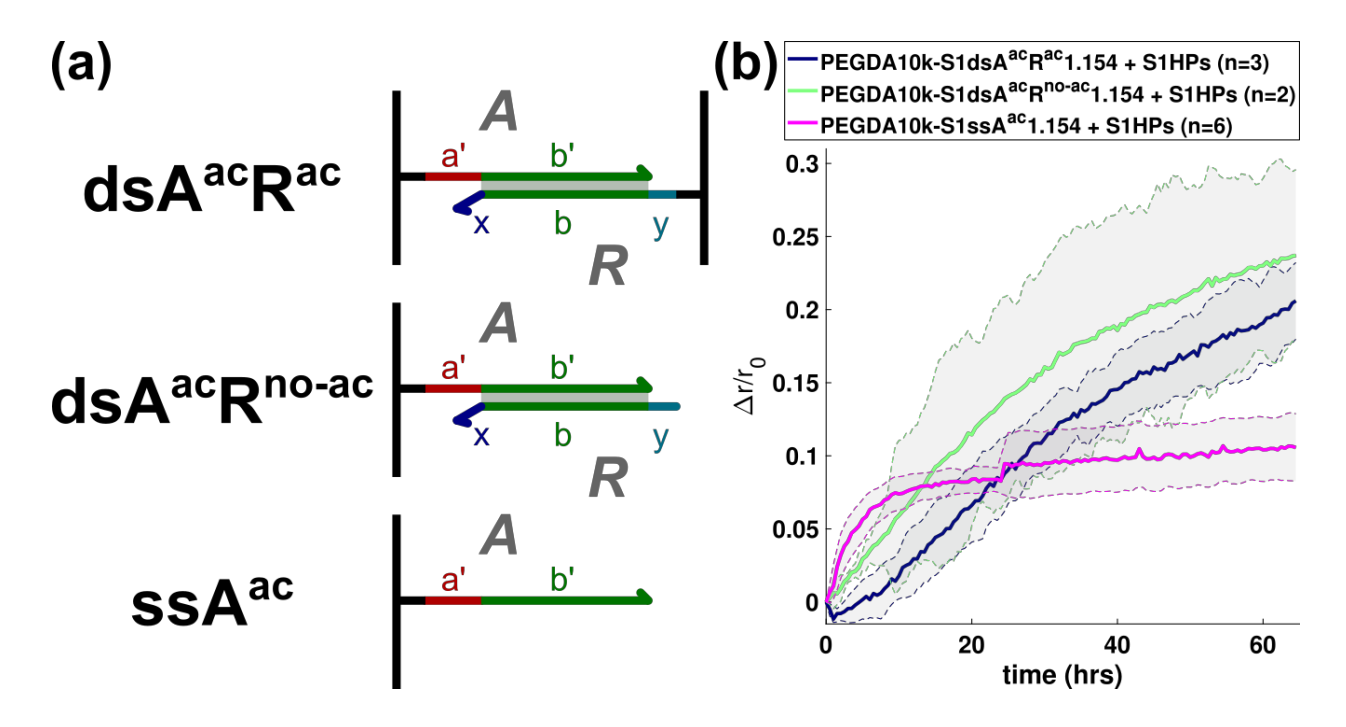
**Supplementary Figure 5**: Relative change in average hydrogel radius of poly(PEGDA10k-*co*-S1dsA<sup>ac</sup>R<sup>ac</sup>1.154) hydrogel particles incubated with varying concentrations of S1 HPs (H1\_S1\_6/3 and H2\_S1\_6/3). The particles were expanded in 1x TAEM. Solid curves are the averages of measurements of the number of particles shown in the legend. Shaded regions show 95% confidence intervals as determined by standard deviations.



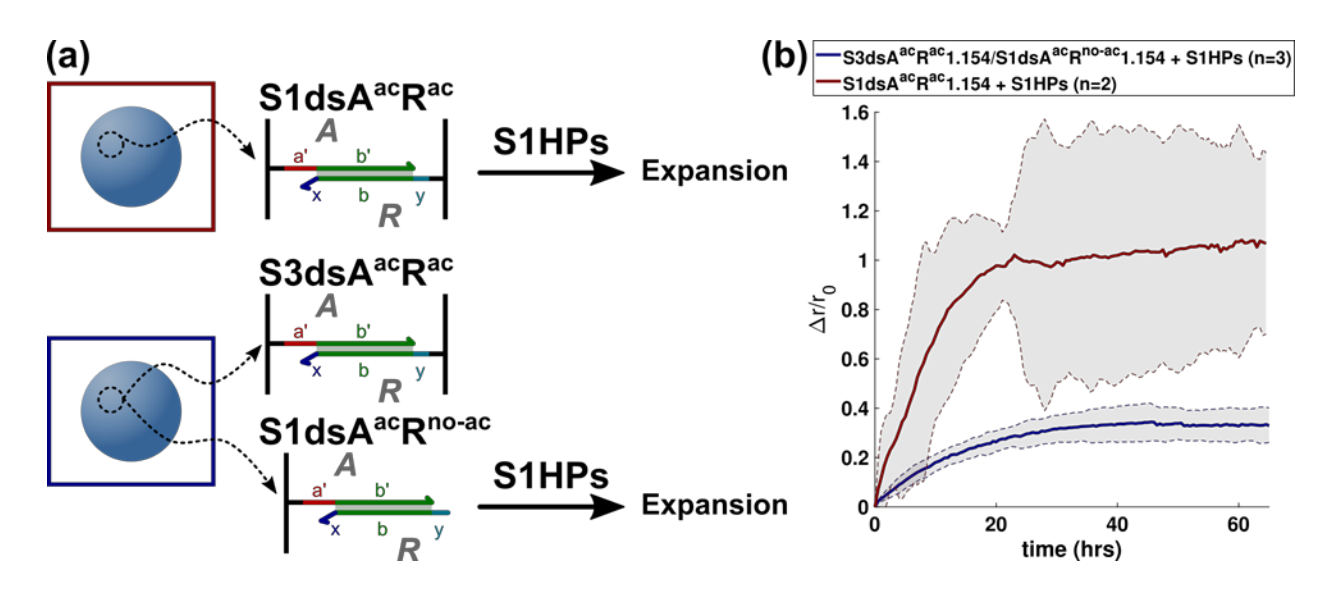
**Supplementary Figure 6**: Relative change in average hydrogel radius of poly(PEGDA10k-*co*-S1dsA<sup>ac</sup>R<sup>ac</sup>1.154) hydrogel particles incubated with 20 μM per hairpin (H1\_S1\_6/3 and H2\_S1\_6/3) in different buffer/salt conditions. Solid curves are the averages of measurements of the number of particles shown in the legend. Shaded regions show 95% confidence intervals as determined by standard deviations. See Supp. Tables 2 and 4 for buffer contents and calculated salt concentrations.



**Supplementary Figure 7**: Relative change in average hydrogel radius of poly(Am-co-S1dsAacRac1.154) hydrogel particles incubated with 20 μM per hairpin (H1\_S1\_6/3 and H2\_S1\_6/3) in different buffer/salt conditions. The fraction of hairpins that were terminator hairpins was 10%. Solid curves are the averages of measurements of the number of particles shown in the legend. Shaded regions show 95% confidence intervals as determined by standard deviations. See Supp. Tables 2 and 3 for buffer contents and calculated salt concentrations. We note that the experiment presented in Figure 4 also utilized 10% terminator hairpins and resulted in an earlier plateau time, which could be attributed to the differences in the polymer network used. The Am-DNA gels are crosslinked solely by modified DNA duplexes and do not have any additional covalent crosslinks, while the PEG-based gels possess a self-crosslinked polymer network that is limited by covalent C-C bonds and can attain swelling equilibrium even without the presence of terminator hairpins.



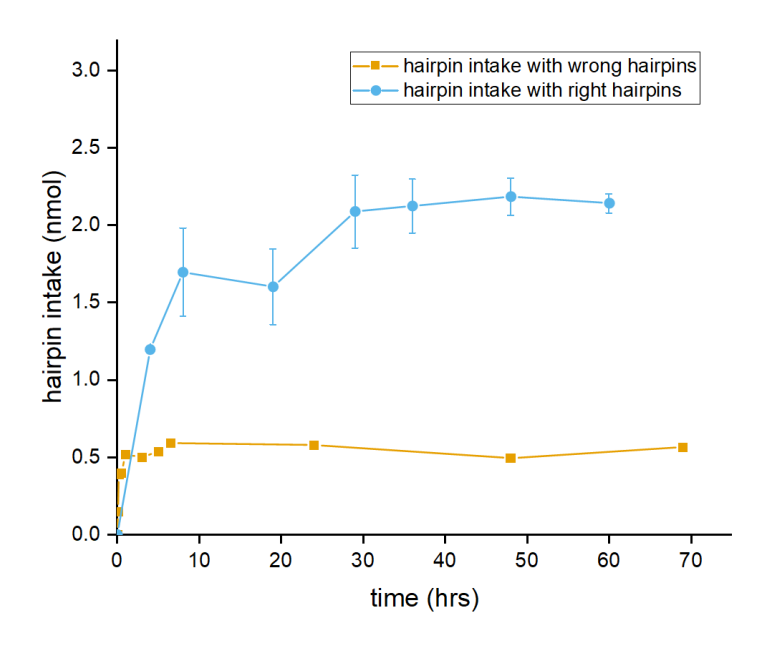
**Supplementary Figure 8**: Expanding poly(PEGDA10k-*co*-S1DNA1.154) particles with different forms of HCR initiators. (a) Methods of integrating DNA into hydrogels. Black lines indicate the polymer backbone. dsA<sup>ac</sup>R<sup>ac</sup> indicates that both sides of the DNA duplex are anchored with the polymer backbone. dsA<sup>ac</sup>R<sup>no-ac</sup> indicates that one side of the DNA duplex is anchored with the polymer backbone through A strand 5′ end. ssA<sup>ac</sup> indicates that only A strand (single strand DNA) is anchored with the polymer backbone through the 5′ end. (b) Relative change in hydrogel radius of hydrogel particles polymerized with the different HCR initiators shown in (a). Hydrogels were expanded with 20 μM sequence set 1 hairpins (H1\_S1\_6/3 and H2\_S1\_6/3). The use of single-stranded HCR initiators(S1ssA<sup>ac</sup>1.154) increased the initial rate of expansion at the expense of a lower final degree of expansion. The particles were expanded in 1x TAEM. Solid curves are the averages of measurements of the number of particles shown in the legend. Shaded regions indicate 95% confidence intervals as determined by standard deviations.



**Supplementary Figure 9**: Expanding DNA-crosslinked polyacrylamide hydrogel particles poly(Am-co-DNA) using different methods of HCR initiation. (a) Schematic showing the DNA integrated into polyacrylamide particles with different HCR initiators. Upper gel: poly(Am-co-S1dsAacRac1.154) hydrogel particles. Lower gel: poly(Am-co-S3dsAacRac1.154-S1dsAacRno-ac1.154) hydrogel particles. In the lower gel, S3dsAacRac1.154, inert to sequence set 1 HPs, was used to simulate the extra binding that S1dsAacRac created in the upper gel. (b) Relative change in hydrogel radius of poly(Am-co-DNA) hydrogel particles polymerized with the double-stranded DNA species shown in (a). The line color corresponds to the box around the hydrogel sphere in (a). Hydrogels were expanded using 20 μM sequence set 1 hairpins (H1\_S1\_6/3 and H2\_S1\_6/3), 10% of which were terminators. In the case of non-crosslinked dsDNA initiator-induced expansion, the hydrogel particles were crosslinked with a second set of DNA crosslinks set 3 with sequences that do not interact with sequence set 1. The particles were expanded in 1x TAEM. Solid curves are the averages of measurements of the number of particles shown in the legend. Shaded regions show 95% confidence intervals as determined by standard deviations.

**Supplementary Text 1**: Note on the Measurement of Hairpin Intake during DNA Polymerization.

To quantify the amount of hairpin intake during a gel swelling process, we first transferred the hairpin solution from the well to a tube at specific time points using a pipette. The total volume of the hairpin solution was then measured using the pipette to prevent errors caused by evaporation. Subsequently, the solution was diluted 100-fold with 1x TAEM, and the absorbance at 260 nm was measured. By referencing the absorbance values to a standard absorbance-concentration curve generated from known concentration hairpin mixtures and taking into account the total volume, we were able to calculate the overall quantity of hairpin present in the solution at a given time point. The hairpin intake was then determined by subtracting this calculated value from the initial amount of hairpins.



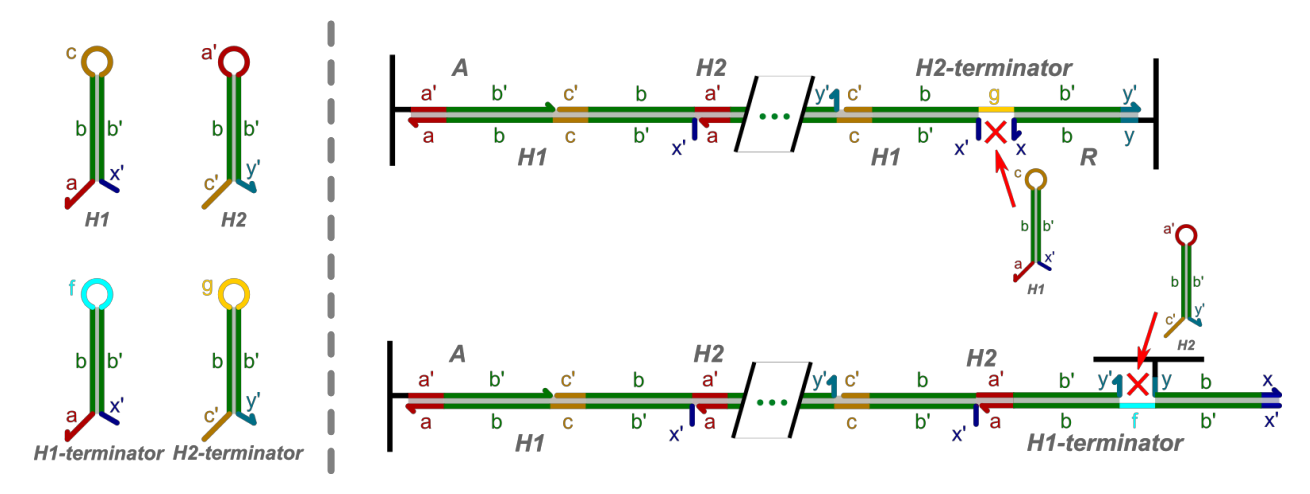
**Supplementary Figure 10**: The relative hairpin intake of poly(PEGDA10k-*co*-S2dsDNA1.154) hydrogel square (1mm side-length, 160 μm thickness) incubated with 60 μM per hairpin in 1xTAEM buffer. We note that this gel used is twice the volume as the triangle-shaped gels used in other studies of this paper and calculations in Supp. Text 1 have been adjusted accordingly. Right hairpins: S2 HPs (H1\_S2\_mb and H2\_S2\_mb, with 1% of H1\_S2\_mb\_ter and H2\_S2\_mb\_ter), which have the correct sequences that can direct gel swelling (n=3); wrong hairpins: S4 HPs (H1\_S4\_mb and H2\_S4\_mb, with 1% of H1\_S4\_mb\_ter and H2\_S4\_mb\_ter), which have the incorrect sequences and not inducing gel swelling (n=1). The intake with incorrect hairpins was used as a baseline for hairpin intake that did not participate in the HCR and was subtracted from the correct hairpin measurement in the above calculation.

We presume the amount of hairpin intake would vary depending on factors such as crosslink concentrations, hairpin design and concentrations, polymer type, etc., and the amount of hairpin intake for these varying parameters would be valuable for understanding mechanistic details. In

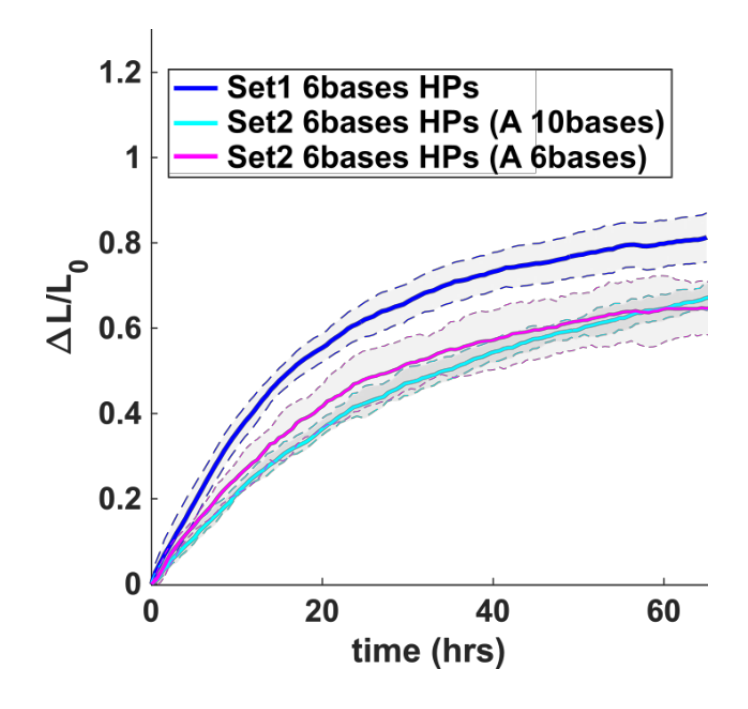
our specific experimental conditions, as shown in Supp. Fig. 10, we found that approximately 0.8 nmol of each type of DNA hairpin was consumed by the gel employed in this study, which had twice the volume of the triangle gels commonly used throughout this paper. Assuming a rough linearity between hairpin intake and crosslink amount, which is proportional to the gel volume, the triangle-shaped gels would exhibit an intake of 0.4 nmol for each type of hairpin. Initially, the DNA crosslinks were present at a concentration of 1.154 mM in the pre-gel solution. Previous studies have reported efficiency of DNA anchoring for acrydite-modified DNA in photopatterned PEG-based gels at approximately 55%. The final DNA anchoring efficiency is therefore approximately 80% by simple calculation of probability as each DNA duplex contains two acrydite-modified groups. Therefore, the final concentration of DNA crosslinks inside the gel is about 0.92 mM. With a gel volume of 0.08  $\mu$ L, the DNA crosslinks inside each gel amounted to 0.07 nmol. Consequently, the number of hairpins inserted for each crosslink point is approximately 12 (6 for each hairpin type).

### **Supplementary Text 2**: Note on the function of terminator hairpins.

To regulate the final degree of swelling in DNA polymerization gels, a novel type of hairpin known as "terminator hairpins" was developed and utilized in conjunction with polymerizing hairpins. As described in <sup>1</sup>, the loop domains (c and a') of the terminator hairpin were altered to contain non-complementary sequences. This modification ensures that when the terminator hairpin is inserted into the crosslink, no monomers can interact with the binding site, thereby providing control over the final degree of swelling.

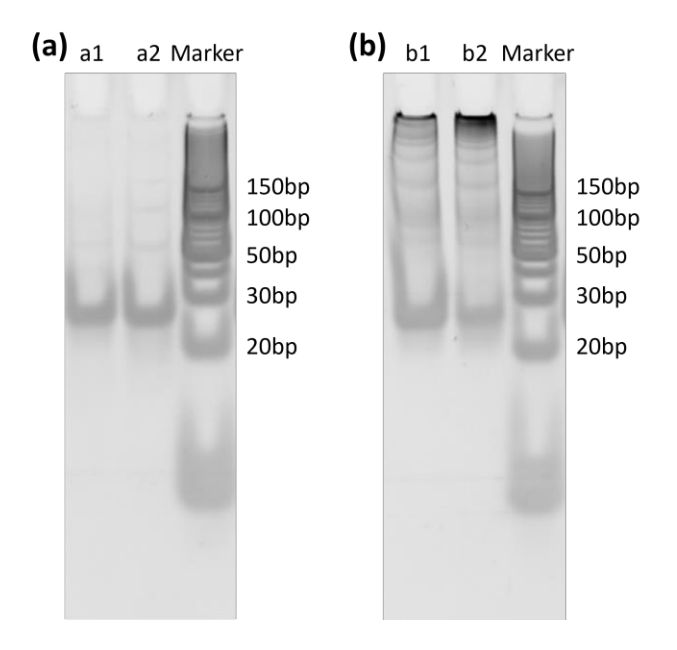


**Supplementary Figure 11**: Schematic of the terminator hairpin creating sites where hairpins can not bind.



Supplementary Figure 12: Swelling comparison between set1 and set2 DNA polymerization gels.

Dark blue: poly(PEGDA10k-co-S1dsDNA1.154) hydrogels incubated with S1 HPs (H1\_S1\_6/3 and H2\_S1\_6/3) in 1x TAEM at 20  $\mu$ M per hairpin type. Light blue: poly(PEGDA10k-co-S2v1dsDNA1.154) hydrogels incubated with S2 HPs (H1\_S2\_6/3 and H2\_S2\_6/3) in 1x TAEM at 20  $\mu$ M per hairpin type. Magenta: poly(PEGDA10k-co-S2v3dsDNA1.154) hydrogels incubated with S2 HPs (H1\_S2\_6/3 and H2\_S2\_6/3) in 1x TAEM at 20  $\mu$ M per hairpin type. Solid curves are the averages of measurements of the number of hydrogels shown in the legend. Shaded regions show 95% confidence intervals as determined by standard deviations.



Supplementary Figure 13: Non-denaturing PAGE gel electrophoresis. Gels were made using 15% acrylamide/bis-acrylamide 19:1 solution in 1xTAEM and were polymerized with 0.5% by volume of 10% APS solution and 0.05% by volume TEMED. Each well contains 12μL of solution with a final concentration of 1 μM of each hairpin type. (a1) H1\_S2\_6/3 (51 bases); (a2) H2\_S2\_6/3 (51 bases); (b1) 0.05μM A\_S2a6 + H1\_S2\_6/3 + H2\_S2\_6/3; (b2) 0.05 μM A\_S2a6 + 0.05 μM R\_S2 (A and R annealed) + H1\_S2\_6/3 + H2\_S2\_6/3. The solutions were prepared and allowed to sit for 3 days to mimic the gel swelling timescale before conducting gel electrophoresis. The gels were run in 1xTAEM buffer for 75 minutes at 150V and stained with 1x Sybr Gold for 15 minutes. The (a) gel shows that the great majority (>95%) of the hairpins remained in the single-strand form (the band observed between the 20 bp and 30 bp bands in the dsDNA ladder land). The faint bands observed traveling the same distance as the 50 bp bands in the dsDNA ladder correspond to the expected size of hairpin dimers but are very faint. The faintness of these bands with respect to the bands corresponding to hairpin monomers suggests that dimerization between hairpins is not a dominant effect driving swelling dynamics. The (b) gel shows that b2)

had a higher degree of polymerization, as indicated by the higher intensity near the loading area.

There was no significant difference in bands near 50 bp, where the hairpins might form dimers.

Together with the experimental findings in Figure 7, we can conclude that the presence of both A+R strands within the hydrogel is crucial to achieving a significant amount of swelling.

**Supplementary Video 1:** The swelling process of poly(PEGDA10k-co-dsDNA1.154) hydrogel triangles polymerized with sequence set 2 v3 DNA crosslinks using sequence set 2 hairpins in 1x TAEM (H1\_S2\_6/3 and H2\_S2\_6/3), the concentration of HPs was total 20  $\mu$ M per hairpin.

**Supplementary Video 2:** The swelling process of poly(Am-co-DNA) gels hydrogel particles polymerized with sequence set 1 DNA crosslinks using sequence set 1 hairpins with 2% terminator strands in 1x TAEM (H1\_S1\_6/3 and H2\_S1\_6/3, H1\_S1\_ter and H2\_S1\_ter), the concentration of HPs was total 20  $\mu$ M per hairpin.

**Supplementary Video 3:** The swelling process of poly(Am-co-DNA) gels hydrogel particles polymerized with sequence set 1 DNA crosslinks using sequence set 1 hairpins with 10% terminator strands in 1x TAEM (H1\_S1\_6/3 and H2\_S1\_6/3, H1\_S1\_ter and H2\_S1\_ter), the concentration of HPs was total 20  $\mu$ M per hairpin.

# **Supplementary References**

- A. Cangialosi, C. Yoon, J. Liu, Q. Huang, J. Guo, T. D. Nguyen, D. H. Gracias and R. Schulman, *Science*, 2017, **357**, 1126–1130.
- 2 J. Fern and R. Schulman, *Nat. Commun.*, 2018, **9**, 1–8.
- S. Venkataraman, R. M. Dirks, P. W. K. Rothemund, E. Winfree and N. A. Pierce, *Nat. Nanotechnol.*, 2007, **2**, 490–494.
- 4 J. N. Zadeh, C. D. Steenberg, J. S. Bois, B. R. Wolfe, M. B. Pierce, A. R. Khan, R. M. Dirks and N. A. Pierce, *J. Comput. Chem.*, 2011, **32**, 170–173.
- 5 R. Shi, J. Fern, W. Xu, S. Jia, Q. Huang, G. Pahapale, R. Schulman and D. H. Gracias, *Small*, 2020, **16**, 2002946.
- R. Owczarzy, B. G. Moreira, Y. You, M. A. Behlke and J. A. Walder, *Biochemistry*, 2008, **47**, 5336–5353.
- R. Shi, K.-L. Chen, J. Fern, S. Deng, Y. Liu, D. Scalise, Q. Huang, N. J. Cowan, D. H. Gracias and R. Schulman, *bioRxiv*, 2022, 2022.09.21.508918.
- 8 M. Rubanov, P. J. Dorsey, D. Scalise and R. Schulman, *ACS Mater. Lett.*, 2022, **4**, 1807–1814.